SUPERHYDROPHOBICITY CAN ENHANCE CONVECTIVE HEAT TRANSFER IN PRESSURE-DRIVEN PIPE FLOW

by HENRY RODRIGUEZ-BROADBENT[†] and DARREN G. CROWDY

(*Department of Mathematics, Imperial College London, London SW7 2AZ, UK*)

[Received 1 January 2022. Revised 26 October 2022. Accepted 27 October 2022]

Summary

Theoretical evidence is given that it is possible for superhydrophobicity to enhance steady laminar convective heat transfer in pressure-driven flow along a circular pipe or tube with constant heat flux. Superhydrophobicity here refers to the presence of adiabatic no-shear zones in an otherwise solid no-slip boundary. Adding such adiabatic no-shear zones reduces not only hydrodynamic friction, leading to greater fluid volume fluxes for a given pressure gradient, but also reduces the solid surface area through which heat enters the fluid. This leads to a delicate trade-off between competing mechanisms so that the net effect on convective heat transfer along the pipe, as typically measured by a Nusselt number, is not obvious. Existing evidence in the literature suggests that superhydrophobicity always decreases the Nusselt number, and therefore compromises the net heat transfer. In this theoretical study, we confirm this to be generally true but, significantly, we identify a situation where the opposite occurs and the Nusselt number increases thereby enhancing convective heat transfer along the pipe.

1. Introduction

In heat transfer engineering, the study of fully developed laminar flow convection in pipes and ducts is a fundamental one of long-standing interest. The Nusselt number is a measure of convective heat transfer, characterised by the difference between the temperature of a flow at its conducting boundary and its mixing cup temperature, at a given axial location. It can be interpreted as inversely proportional to the convective resistance of a flow which, in addition to the caloric resistance, constitutes the full thermal resistance of a flow (**1**). It is therefore often desirable to increase the Nusselt number so as to promote the removal of heat in the system by the fluid. Examples range from typical heat exchangers to cooling systems in microelectronic devices such as laptop computers. In 1971, Shah and London (**2**) compiled a comprehensive survey of known solutions, in the so-called fully developed situation, for the laminar flow and temperature profiles, and heat transfer coefficients (the Nusselt number) in uniform pipes of different cross-sectional shapes. One of the simplest cases of laminar flow along a circular pipe of uniform cross-section and with a constant heat flux entering the fluid uniformly through the no-slip circular boundary is known to have a Nusselt number $\mathrm{Nu} = 48/11$.

In surface engineering, on the other hand, a class of surfaces described as superhydrophobic (**3** to **5**) has been receiving increasing attention, owing to the fact that they can dramatically reduce

[†]Corresponding author<hjr20@ic.ac.uk>

Q. Jl Mech. Appl. Math, Vol. 75. No. 4 © The Author, 2022. Published by Oxford University Press.

https://doi.org/10.1093/qjmam/hbac016

flow resistance. This is a result of capillary effects that allow a surface microstructure to support interfaces, or menisci, that prevent fluid from fully penetrating interstitial regions between pillars, posts or gratings, leading to trapped gas pockets and enhanced slip over the spanning menisci. Maintaining and controlling this so-called Cassie state remains a key challenge for the successful deployment of superhydrophobic surfaces in applications and is a subject of active ongoing research (**5**).

The implications for heat transfer of superhydrophobic surfaces are a subject of burgeoning interest. Making the boundary of a pipe 'superhydrophobic' by adding no-shear regions creates a trade-off in the context of convective heat transfer: the presence of free surfaces, which are generally treated as adiabatic, reduces the area of contact between fluid and boundary through which heat conduction occurs and this can reasonably be expected to decrease the efficacy of heat transfer; on the other hand, those same free surfaces generally increase the fluid flow rate by reducing hydrodynamic friction suggesting that any heat entering the system is advected downstream more efficiently. While it is clear that the improved flow rate alone reduces the caloric resistance of the flow (**1**), the net effect on convective resistance and therefore the Nusselt number is not obvious and has been a topic of recent investigation. So far, the consensus from the wider experimental and theoretical literature is that superhydrophobicity does not typically lead to increased Nusselt numbers: that is, the loss of surface area for heat conduction is not mitigated by the enhanced advection leading overall to less effective convective heat transfer. Consequently, at the time of writing, early hopes that superhydrophobicity might be a boon for convective heat transfer appear to be misplaced.

The present paper has been inspired by an important recent paper by Kirk *et al.* (**6**) which studied the thermally fully developed flow along a channel between two superhydrophobic surfaces where heat enters the fluid along the no-slip portions of the boundary walls with constant heat flux, but not through an array of no-shear slots that decorate the walls and enhance the hydrodynamic slip. The aim of Kirk *et al.* (**6**) was to extend the earlier work of Maynes *et al.* (**7**) and Maynes and Crockett (**8**) who were the first to investigate the Nusselt number mathematically in such a channel geometry. A distinction is that Kirk *et al.* (**6**) solve the mixed boundary value problem for the flow rather than relying, as did the earlier authors, on an effective Navier-slip boundary condition to model the heterogeneous surface and which leads to simpler boundary value problems for both the flow and the temperature fields. Kirk *et al.* (**6**) also relax the assumption that the no-shear slots are flat, and flush with the no-slip surface, in order to investigate the effect of meniscus curvature on the heat transfer properties. This work was motivated by similar theoretical work examining the effect of meniscus curvature on hydrodynamic slip by Sbragaglia and Prosperetti (**9**) and Crowdy (**10**). It is worth mentioning that there are similarities with mass transfer problems; Haase and Lammertink (**11**) have studied heat and mass transfer problems in channel geometries focusing mainly on the transverse flow case where the pressure gradient drives flow across the grooves, rather than the case of longitudinal flow along the grooves.

It turns out that analytical solutions exist for the velocity field associated with pressure-driven longitudinal flow along a pipe whose circular boundary has a regular array of no-shear slots, m such slots say, interspersed with no-slip zones (Fig. 1); the solutions to boundary value problems relevant to such a flow were derived by Philip (**12**) albeit in a different physical context. The heat transfer problem in Philip's superhydrophobic pipe does not appear to have been investigated before and is the focus of the present paper. Like Kirk *et al.* (**6**), we examine the full mixed boundary value problem and avoid making any Navier-slip approximation. For now, however, we assume that the meniscus curvature is the same as the solid boundary so that the shape of the global pipe boundary is still a circle, albeit now with boundary conditions of mixed type imposed on it. We also simplify

conditions along the meniscus by neglecting the effects of evaporation and condensation, and of thermocapillary stresses, both of which have been previously studied (**13**, **14**).

Incidentally, Philip's pipe flow solutions have recently been extended by Crowdy (**15**) who found generalized analytical solutions for flow in superhydrophobic pipes with an annular cross-section and no-shear patterning on one of the two boundary walls. The heat transfer properties of those flows are also of interest and will be studied in future work.

Our main finding here is that while a cylindrical tube with $m > 1$ slots follows the trend of previous literature of having a reduced Nusselt number compared to a fully no-slip boundary, the single-slot case $m = 1$ deviates from this and, in fact, leads for a range of slot sizes to an enhanced Nusselt number. This surprising result is demonstrated theoretically by using complex variable methods to solve the laminar flow boundary value problems for the temperature field. From these, it is a simple matter to calculate diagnostic quantities such as the mass and enthalpy flux rates and the Nusselt number. On an applied mathematical note, the methods of complex analysis and conformal mapping which we espouse here are not commonly used in studying heat transfer problems although their relevance and usefulness in this context is known (**16**).

A second key result of this article stems from a matched asymptotic analysis in the many-slot limit. This yields an expression for the first-order correction to the Nusselt number from the familiar value of $48/11$ associated with the fully no-slip boundary.

The structure of the article is as follows. The mathematical formulation is presented in section 2. Section 3 then gives details of the complex variable methods used to solve for the velocity and temperature fields in the fully developed flow scenario. The Nusselt number is defined in section 4 and the use of the complex form of Stokes theorem to compute several important integral quantities is discussed. The main Nusselt number calculations are presented in sections 5 and 6, and a discussion of the implications of these results is given in section 7. Many of the more technical details have been relegated to a set of appendices for clarity of exposition.

2. Mathematical formulation

We consider fully thermally developed (**17**), steady, unidirectional, incompressible, laminar flow through a cylindrical tube or pipe, with $m \geq 1$ azimuthally periodic, longitudinal slots, held in Cassie state as proposed by Lam *et al.* (**1**). The tube cross-section is a circular disc of radius $\mathcal{R}$ and is assumed to sit in an (x^*, y^*) plane with Z^* taken as the axial coordinate, in the direction of the flow. (We have avoided use of z since later it will denote the complex variable $z = x + iy$; note also that starred variables indicate dimensional quantities, not complex conjugate quantities which will later be denoted using overbars). As shown in Figs 2 and **??**, θ/m is defined as half the solid angle subtended at the centre of the pipe by each no-slip ridge, parametrising the arclength of contact between the fluid and the boundary for each geometry, and therefore the size of menisci as well. A no-slip condition holds where the fluid is in contact with the ridge top, and a no-shear condition holds on the meniscus (held above what we assume to be vapour-filled grooves (**18**)). In this steady unidirectional flow scenario the three-dimensional Navier–Stokes equations for a fluid with constant viscosity μ, axial pressure gradient $\partial p/\partial Z^*$ and axial velocity $w^*(x^*, y^*)$ simplify to

$$\frac{\partial p}{\partial Z^*} = \mu \left(\frac{\partial^2 w^*}{\partial x^{*2}} + \frac{\partial^2 w^*}{\partial y^{*2}} \right). \tag{2.1}$$

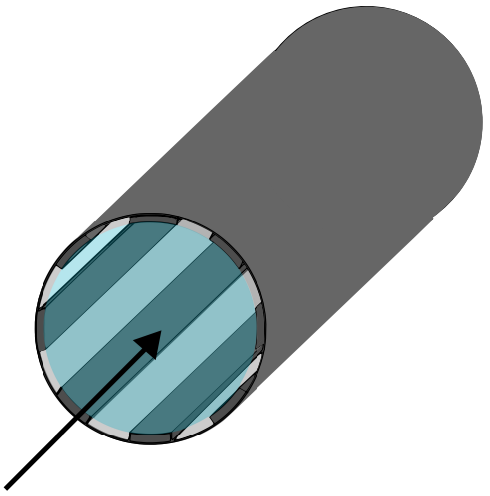

Fig. 1 Fluid flow along a superhydrophobic tube. The surface of the tube is patterned by a regular array of $m \geq 1$ no-shear slots. The slots reduce not only the hydrodynamic friction but also the surface area for heat conduction into the fluid, making the effect on the Nusselt number unclear.

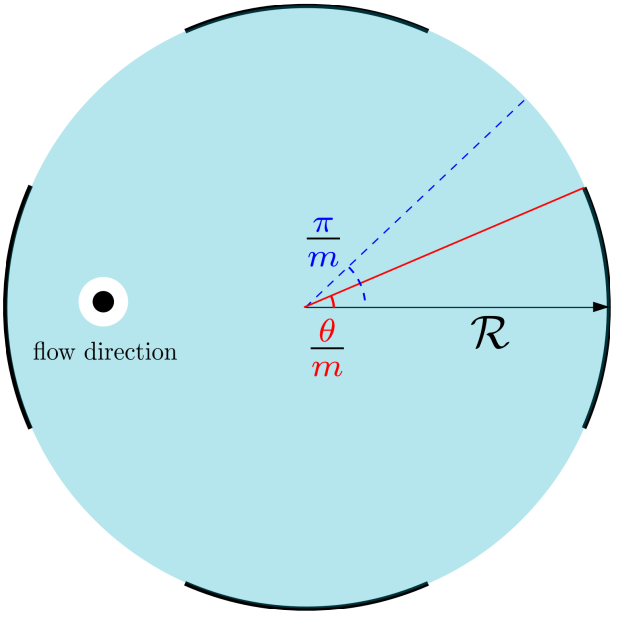

Fig. 2 A cross-section of the tube in the case $m = 4$; the Z^* direction is taken 'into' the page. The ratio θ/π is the fraction of the boundary where a no-slip condition holds.

Define unstarred, dimensionless variables, and calligraphic dimensional scales:

$$x^* = \mathcal{R}x, \qquad y^* = \mathcal{R}y, \qquad w^* = \mathcal{W}w, \tag{2.2}$$

and choose that

$$\mathcal{W} = -\frac{\mathcal{R}^2}{\mu}\frac{\partial p}{\partial Z^*}; \tag{2.3}$$

the negative sign is included in consistency with the literature, as $\partial p/\partial Z^*$ is taken to be a negative constant, so that the dimensionless flow goes 'into' the page. The dimensionless governing equation is then of Poisson type,

$$\nabla^2 w = -1, \tag{2.4}$$

where ∇^2 denotes the two-dimensional (2D) Laplacian. The no-slip and no-shear boundary conditions are then

$$\begin{aligned} w &= 0 \text{ on the no-slip ridges,} \\ \frac{\partial w}{\partial n} &= 0 \text{ on the no-shear menisci.} \end{aligned} \tag{2.5}$$

The notations $\partial/\partial s$ and $\partial/\partial n$ refer to tangential and fluid-inward normal derivatives around the boundary, respectively, where s increases with the fluid region to the left as the boundary is traversed.

Now consider the thermal problem. For a fluid with thermal conductivity k, specific heat under constant pressure c_p and density ρ, the dimensional temperature T^* is governed by the advection–diffusion equation (**17**)

$$k\left(\frac{\partial^2 T^*}{\partial x^{*2}} + \frac{\partial^2 T^*}{\partial y^{*2}}\right) = \rho c_p w \frac{\partial T^*}{\partial Z^*}, \tag{2.6}$$

where the unidirectional and fully developed assumptions have simplified the advection and diffusion terms, respectively. Conduction with constant heat flux per unit area q''_{sl} through the wetted perimeter is modelled by the boundary condition

$$-k\frac{\partial T^*}{\partial n^*} = \begin{cases} q''_{sl}, & \text{on the no-slip ridges,} \\ 0, & \text{on the no-shear menisci.} \end{cases} \tag{2.7}$$

The thermally developed assumption gives that $\partial T^*/\partial Z^*$ is constant (**17**), so by similarly defining dimensionless temperature T such that $T^* = \frac{\mathcal{R}q''_{sl}}{k}T$, and introducing the dimensionless parameter $P = \frac{\mathcal{R}\rho c_p}{\mathcal{W}q''_{sl}}\frac{\partial T^*}{\partial Z^*}$, the dimensionless advection–diffusion equation is

$$\nabla^2 T = Pw, \tag{2.8}$$

with boundary conditions

$$-\frac{\partial T}{\partial n} = \begin{cases} 1, & \text{on the no-slip ridges,} \\ 0, & \text{on the no-shear menisci.} \end{cases} \tag{2.9}$$

3. Solutions for the velocity and temperature profiles

It is convenient to introduce the complex coordinate $z = x + iy$ as the coordinate in the flow cross-section and write the axial velocity profile as a function of this variable and its complex conjugate $\bar{z}$, that is, $w = w(z, \bar{z})$. The no-slip and no-shear boundary conditions (2.5) are then stated as

$$\begin{aligned} w = \frac{\partial w}{\partial s} &= 0 \text{ for } |z| = 1, \, |\arg(z^m)| < \theta, \\ \frac{\partial w}{\partial n} &= 0 \text{ for } |z| = 1, \, |\arg(z^m)| > \theta, \end{aligned} \tag{3.1}$$

where the argument is taken as $\arg(z) \in (-\pi, \pi]$. Philip (**12**) has given the solution to this flow problem. Rephrased in present notation, it is

$$w(z, \bar{z}) = \frac{1}{4}(1 - z\bar{z}) + \frac{1}{m}\mathrm{Im}\left[\cos^{-1}\left\{\frac{\cos\left(-\frac{im}{2}\log((-1)^{1/m}z)\right)}{\cos\frac{\pi-\theta}{2}}\right\} + \frac{im}{2}\log((-1)^{1/m}z)\right], \tag{3.2}$$

which can be rewritten as

$$w(z, \bar{z}) = \frac{1}{4}\left(1 - z\bar{z} + f(z) + \overline{f(z)}\right), \tag{3.3}$$

where $f(z)$ is the holomorphic function

$$f(z) = \frac{2}{m}\left(\log\left(1 - z^m + \sqrt{z^{2m} - 2z^m\cos\theta + 1}\right) - \log\left(2\sin\frac{\theta}{2}\right)\right). \tag{3.4}$$

This expression differs from that given by Philip (**12**) but proves convenient for present purposes.

With this result at hand, the temperature problem can then be stated in complex variable form as

$$\frac{\partial^2 T}{\partial z \partial \bar{z}} = \frac{P}{16}\left(1 - z\bar{z} + f(z) + \overline{f(z)}\right), \tag{3.5}$$

which is readily solved by

$$T(z, \bar{z}) = \frac{P}{16}\left(z\bar{z} - \frac{z^2\bar{z}^2}{4} + \bar{z}F(z) + z\overline{F(z)}\right) + g(z) + \overline{g(z)}, \tag{3.6}$$

where

$$F(z) \equiv \int_0^z f(\hat{z})d\hat{z}, \tag{3.7}$$

and $g(z)$ is a holomorphic function to be determined by enforcing the boundary conditions (2.9) which can be restated as

$$-\frac{\partial T}{\partial n} = \begin{cases} 1, & \text{for } |z| = 1, \, |\arg(z^m)| < \theta, \\ 0, & \text{for } |z| = 1, \, |\arg(z^m)| > \theta. \end{cases} \tag{3.8}$$

Further, by integrating the governing equation over the domain we find that

$$P = \frac{16\theta}{\pi\left(1 - \frac{8}{m}\log\sin\frac{\theta}{2}\right)} \tag{3.9}$$

which can be viewed as a conservation of energy result. Due to the assumption of a thermally fully developed flow, this solution is unique up to a constant that depends on the axial coordinate (**17**), so without loss of generality we impose

$$T(0,0) = 0. \tag{3.10}$$

We find the solution to the temperature problem (the details are in Appendix A) to be

$$\begin{aligned} T(z,\bar{z}) =& \frac{P}{16}\left(z\bar{z} - \frac{z^2\bar{z}^2}{4} + (1+z\bar{z})\left(\frac{F(z)}{z} + \frac{\overline{F(z)}}{\bar{z}}\right) - 2f(0)\right) \\ &+ \mathrm{Re}\left[\frac{i}{\pi m}\left(\mathrm{Li}_2\left(z^m e^{-i\theta}\right) - \mathrm{Li}_2\left(z^m e^{i\theta}\right)\right) - \frac{P}{4}\left(\int_0^z \frac{f(\hat{z}) - f(0)}{\hat{z}}d\hat{z}\right)\right], \end{aligned} \tag{3.11}$$

where Li_2 is the dilogarithm (**19**). Note that in the special case that $m = 1$:

$$\begin{aligned} F(z)|_{m=1} =& zf(z) + \sqrt{z^2 - 2z\cos\theta + 1} \\ &+ 2\cos^2\frac{\theta}{2}\log\frac{z - \cos\theta + \sqrt{z^2 - 2z\cos\theta + 1}}{1 - \cos\theta} - z - 1, \end{aligned} \tag{3.12}$$

although this is the only case for which any of the indefinite integrals in (3.11) can be expressed in terms of elementary functions.

4. The Nusselt number

The Nusselt number is a convenient quantifier of the benefit to convective heat transfer attained by using a superhydrophobic surface (**6, 18, 20** to **23**) with the value for a fully no-slip cylindrical tube well known to be the benchmark 48/11. To define the Nusselt number, we first define the mixing cup temperature of the flow, T_b (**17**) to be

$$T_b = \frac{\iint_{\text{pipe}} wT dA}{\iint_{\text{pipe}} w dA}. \tag{4.1}$$

This quantity characterises the temperature of the bulk flow. In an unbounded system the far-field temperature is typically used, however in bounded systems such as that considered here, this weighted average of the fluid temperature is preferred (**6**, **17**). The local Nusselt number, $\mathrm{Nu}(z)$, is the ratio of cooling through all mechanisms to cooling through convection alone at a particular boundary point (**8**), so on the boundary $|z| = 1$ it is defined as

$$\mathrm{Nu}(z) = \frac{h(z)D}{k}, \tag{4.2}$$

where $h(z) = \frac{q''_{sl}}{T^*-T^*_b}$ is the Newton cooling coefficient (and $T^*_b = \frac{\mathcal{R}q''_{sl}}{k}T_b$), and $D = 2$ is the hydraulic diameter. Consequently, for present purposes this simplifies to

$$\mathrm{Nu}(z) := \begin{cases} \frac{2}{T(z)-T_b}, & \text{for } |\arg(z^m)| < \theta, \\ 0, & \text{for } |\arg(z^m)| > \theta. \end{cases} \tag{4.3}$$

In order to characterise each geometry in a more general sense, the average Nusselt number $\overline{\mathrm{Nu}}$, is defined as

$$\overline{\mathrm{Nu}} := \frac{1}{2\pi}\int_{-\pi}^{\pi} \mathrm{Nu}(e^{is})ds. \tag{4.4}$$

4.1 *Integral Quantities*

The complex form of Stokes' theorem says that, given a domain D with boundary ∂D, and a function Φ regular in D, then

$$\iint_D \frac{\partial \Phi}{\partial \bar{z}} dA = \frac{1}{2i}\oint_{\partial D} \Phi dz. \tag{4.5}$$

This, and its complex conjugate form, can be used to efficiently determine the mass and enthalpy flux rates. Indeed it can be shown that

$$Q(\theta, m) := \iint_{|z|<1} w dA = \frac{\pi}{8}\left(1 - \frac{8}{m}\log\sin\frac{\theta}{2}\right), \tag{4.6}$$

matching Philip's result (**24**). Similarly, for the enthalpy flux rate $H(\theta, m)$:

$$\begin{aligned} H(\theta, m) &:= \iint_{|z|<1} wT dA \\ &= \frac{\theta}{4\left(1 - \frac{8}{m}\log\sin\frac{\theta}{2}\right)}\left(\frac{7}{48} - \frac{7}{3m}\log\sin\frac{\theta}{2} + \frac{8}{m^2}\left(\log\sin\frac{\theta}{2}\right)^2\right) \\ &\quad + \sum_{n=1}^{\infty}\left(\frac{a_n \sin n\theta}{2mn^2(mn+1)} - \frac{\theta a_n^2}{2\left(1 - \frac{8}{m}\log\sin\frac{\theta}{2}\right)}\frac{3mn+4}{mn(mn+1)^2(mn+2)}\right), \end{aligned} \tag{4.7}$$

where a_n are the Taylor coefficients of $f(z)$, that is:

$$f(z) = \sum_{n=0}^{\infty} a_n z^{mn}. \tag{4.8}$$

The details of these calculations are included in Appendix B. Equations (4.6) and (4.7) provide useful formulas for Q and H from which $T_b = H/Q$ can be readily calculated without the need to perform any area integrals over the pipe cross-section.

As described by (4.3) and (4.4), we now can calculate each of the quantities on which the Nusselt number depends. This is done in section 5.

4.2 *Axial temperature gradient*

With the velocity and temperature fields in the cross-section now found, the energy balance described by (3.9) determines the axial temperature gradient along the tube as

$$\frac{\partial T^*}{\partial Z^*} = \frac{16 q''_{sl} \theta}{\rho c_p \pi \left(1 - \frac{8}{m} \log \sin \frac{\theta}{2}\right)} \frac{\mathcal{W}}{\mathcal{R}}. \tag{4.9}$$

5. Nusselt numbers: $m \in O(1) - O(10)$

With the flow and temperature fields determined, the Nusselt number can now be calculated as a function of the slot number m and any θ, representing the solid fraction of the tube boundary.

Our principal interest is in assessing whether there is any advantage to convective heat transfer in using this family of superhydrophobic pipes, over a fully no-slip tube. To make this comparison, we must first establish this benchmark. While the result for this Poiseuille flow is well known (**17**) and was mentioned earlier, we can set $\theta = \pi$ in the solutions here to recover the Nusselt number for the fully no-slip tube:

$$\mathrm{Nu}|_{\theta=\pi} = \frac{48}{11}. \tag{5.1}$$

Replacing the fully no-slip boundary with longitudinal ridges held in the Cassie state can be expected to impact the Nusselt number, that is, the ratio of convective and conductive mechanisms for heat transfer, in two ways. On the one hand, reducing contact between the fluid and the boundary reduces the surface area over which conduction can occur; on the other hand, this diminished contact reduces the drag that the tube exerts on the fluid, increasing the mass flux and thus improving convection (**20**). As already mentioned, the net effect on the Nusselt number is therefore not obvious without a detailed calculation.

Existing evidence in the literature where channel flows have been the focus (**6**, **8**) shows that punctuating a fully no-slip boundary with superhydrophobic ridges can increase the local Nusselt number at points in certain configurations, typically at the triple contact point at the edge of a ridge, however ultimately it decreases the average Nusselt number. Figure 3 shows that this feature is confirmed for the pipe flow scenario provided $m > 1$. However, interestingly, the calculation for $m = 1$ deviates from this trend: it is found that for a range of values of large θ near π, the average Nusselt number $\overline{\mathrm{Nu}}$ *increases* relative to the fully no-slip case. It is also found that there is a finite range of θ for which $\overline{\mathrm{Nu}}$ becomes singular. Such singular behaviour occurs when, at some point on the no-slip boundary, the tube reaches the mixing cup temperature. Numerically we determine that when $m = 1$, this singular behaviour occurs in the range $0.7373\pi < \theta < 0.8939\pi$. Physically, this corresponds to points on the boundary over which there is no conduction, so that the ratio of convection to conduction becomes infinite. For $0.8939\pi < \theta < \pi$, however, the average Nusselt number for a pipe with a single slot $m = 1$ is both well defined and higher than $48/11$.

It should also be pointed out that Fig. 3 is the analogue of Figure 7a in Kirk *et al.* (**6**). For increasing m, it bares a strong resemblance to their figure for increasing h, except in the $m = 1$ case, where we see the surprising improvement in $\overline{\mathrm{Nu}}$.

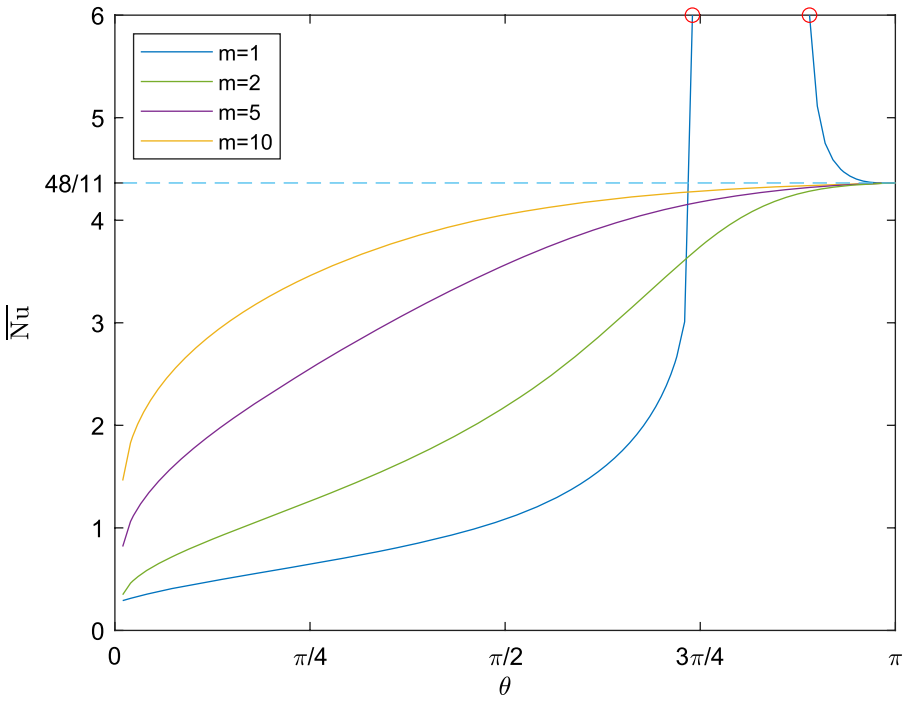

Fig. 3 Average Nusselt number, $\overline{\mathrm{Nu}}$, as a function of solid ridge angle θ: calculated by truncating ten terms in the series for H. For $m = 1$, there is a range of angles θ where $\overline{\mathrm{Nu}}$ is undefined, and a range just below π where $\overline{\mathrm{Nu}}$ is enhanced above the $48/11$ value for a fully no-slip pipe.

6. Nusselt numbers: $m \to \infty$

The many-slot limit, $m \to \infty$, is also of interest. Appendix C gives details of the derivation of asymptotic expansions of the velocity and temperature fields in terms of increasing powers of $1/m$. In this limit, the first-order correction term to the fully no-slip local Nusselt number, $\mathrm{Nu}_\infty(z)$, for $|z| = 1$ is found to be

$$\mathrm{Nu}_\infty(z) = \frac{48\pi}{11\theta} - \frac{1}{m}\frac{1152\pi}{121\theta}\left(2\log\sin\frac{\theta}{2} + \frac{1}{\theta}\mathrm{Im}\left[\mathrm{Li}_2(z^m e^{i\theta}) - \mathrm{Li}_2(z^m e^{-i\theta})\right]\right) + O\left(\frac{1}{m^2}\right), \quad (6.1)$$

where Li_2 is the dilogarithm (**19**), and the analogous result for the average Nusselt number, $\overline{\mathrm{Nu}}_\infty$, is that

$$\overline{\mathrm{Nu}}_\infty = \frac{48}{11} + \frac{1}{m}\frac{576}{121}\left(\frac{1}{\theta^2}\mathrm{Re}\left[\mathrm{Li}_3(e^{2i\theta}) - 2\mathrm{Li}_3(1) + \mathrm{Li}_3(e^{-2i\theta})\right] - 4\log\sin\frac{\theta}{2}\right) + O\left(\frac{1}{m^2}\right), \quad (6.2)$$

where Li_3 is the trilogarithm (**19**). It is interesting that the coefficient of this first-order correction in $1/m$ can be found as a function of θ in analytical form. This coefficient is plotted against θ in Fig. 4 and, being negative over the range of θ values, corroborates that adding a large number of no-shear slots to flow in circular pipe will always be to the detriment of the Nusselt number.

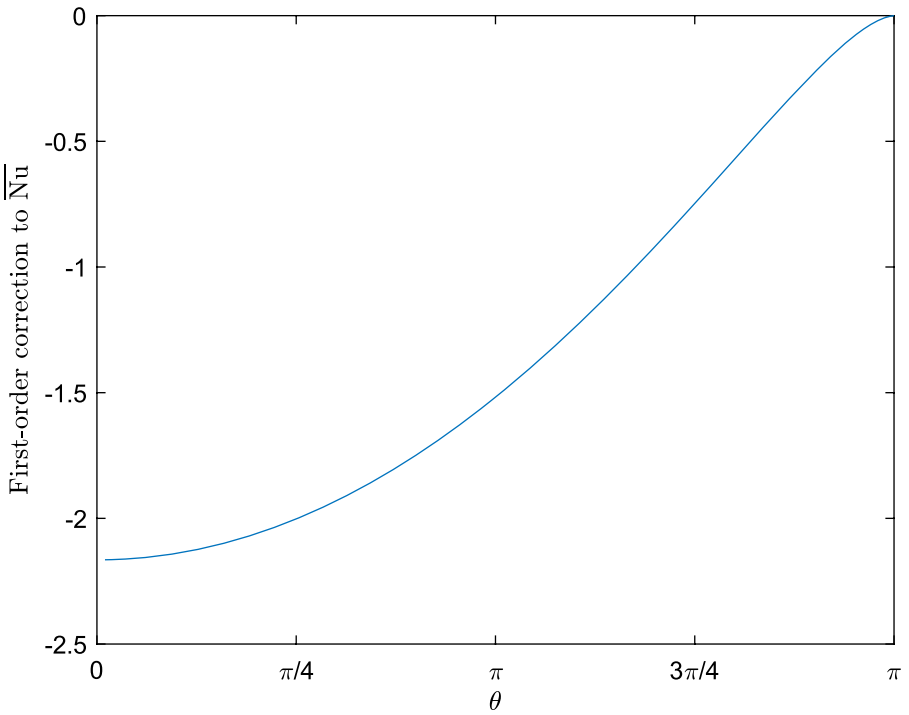

Fig. 4 Coefficient of the first-order correction, as an expansion in $1/m$, of the average Nusselt number plotted against solid ridge angle θ.

Comparing (6.2) against the exact average Nusselt number for a given m shows that this approximation breaks down for smaller values of θ. The size of the range of values of θ for which it is a good approximation is larger for bigger values of m. This is illustrated in Fig. 5. This is an encouraging result for the applicability of this formula: smaller menisci (that is, larger values of θ) are more typically seen in this family of surfaces, owing to increased meniscus stability and the consequent ease in maintaining the Cassie state that underpins the technology.

7. Discussion

The primary result of this article is the discovery of a family of superhydrophobic pipe designs that cause a marked improvement to the Nusselt number compared to a fully no-slip pipe. This is a departure from the consensus to date that superhydrophobicity always lowers the Nusselt number in a given pipe geometry compared to the fully no-slip scenario.

Some intuition on this phenomenon can be gained by studying Fig. 6. The fluid along the solid ridge shows much greater temperature variation in the top row of figures associated with the $m = 1$ case than in the others: note that the contours adjacent to the solid, heated boundary are hot relative to the flow for $m > 1$, while for $m = 1$, $\theta = 4\pi/5$ the contours adjacent to the solid boundary span a wider range of cooler temperatures. The Nusselt number is a ratio of cooling via all mechanisms to cooling via conduction alone (that is, Newton cooling to Fourier cooling (**17**)) and when the

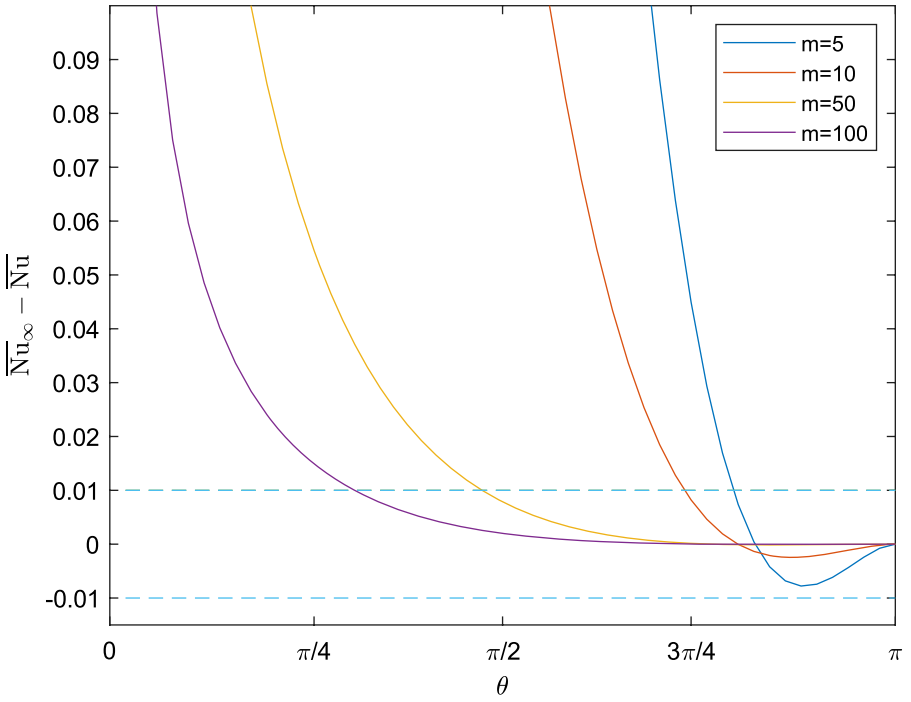

Fig. 5 The error for approximation (6.2), plotted for a range of values of m. The domain of θ with 10^{-2} accuracy, indicated by dashed lines, is seen to grow with m.

fluid temperature at the boundary reaches the mixing cup temperature, the local Newton cooling coefficient, typically denoted by h as in (4.2), blows up; this is illustrated explicitly in Fig. 7 for the configurations in the first row of Fig. 6. In the range of θ where the singular behaviour occurs (which includes the case $\theta = 4\pi/5$), this variability means that that fluid in contact with the boundary reaches cooler temperatures than that seen for other parameter values, making it possible for this fluid to reach the mixing cup temperature. At this point, the Nusselt number denominator in (4.3) approaches zero, resulting in the observed singular behaviour.

This singularity in the Nusselt number should not be considered too seriously: it is not a physical singularity, it merely signifies that the defined diagnostic quantity has reached a limitation, at least in its current mathematical definition, for this class of problem (**6**). The same blow-up of the Nusselt number as defined herein has been observed in other heat transfer problems (**25**). A common fix is to define other measures of convective heat transfer that do not blow up in the same way: Enright *et al.* (**18**) consider one such alternative measure, which is shown to have its own challenges with singularities for this problem in Appendix D. Our conjecture is that while the average Nusselt number introduced here becomes undefined for angles in this range, this very failure might still be expected to be a signature of enhanced convective heat transfer, at least for the larger angles within this range. Indeed, as already pointed out, there is a range of angles close to π where the average Nusselt number is well defined *and* larger than $48/11$.

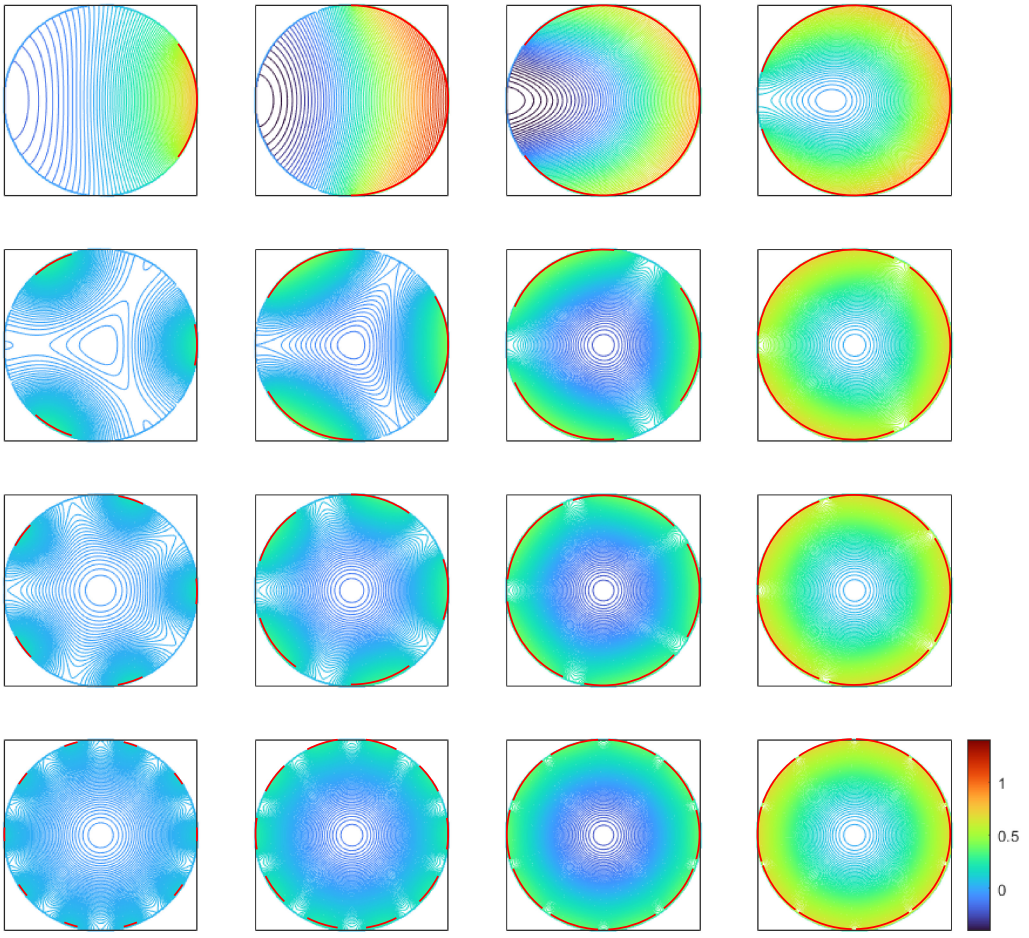

Fig. 6 Temperature contours $(T - T_b)$: left-right: $\theta = \frac{\pi}{5}, \frac{\pi}{2}, \frac{4\pi}{5}, \frac{9\pi}{10}$; top-bottom: $m = 1, 3, 5, 10$. Solid lines at the boundary indicates where heat enters the pipe.

There are practical engineering matters to be considered in building a superhydrophobic pipe of the kind shown here to increase the Nusselt number, since the single slot case features the least robust Cassie state, which in turn typically increases caloric resistance. Nevertheless, this results of this article may rekindle interest in the use of suitably designed superhydrophobic pipes for enhanced convective heat transfer. The same increase in Nusselt number can be expected for other pipe cross-sections leaving open for future investigation the question of designing a practically viable one.

This study has focused on solving the full mixed-type boundary value problem in preference to use of any homogenised Navier-slip 'effective' boundary condition. But it is worth pointing out that, from the matched asymptotics in Appendix C, the outer solution (C. 3) is indeed found to be one corresponding to enforcing such an effective Navier-slip condition, thereby underpinning the use of such approximations in this limit.

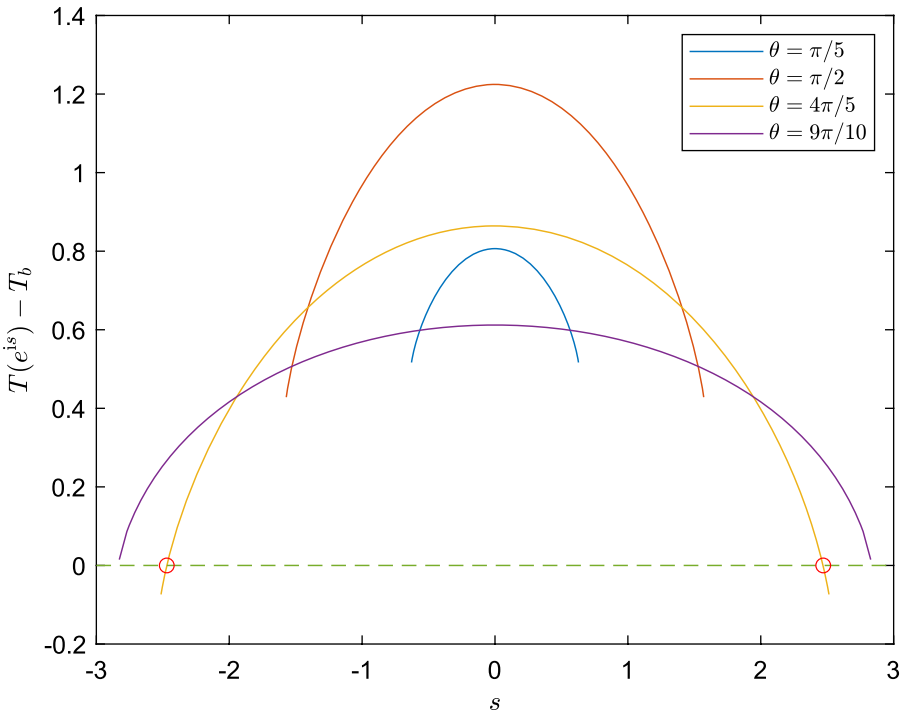

Fig. 7 The difference between the fluid temperature and mixing cup temperature, along the portion of the pipe boundary that conducts heat, in the case $m = 1$ for the range of values of θ featured in the first row of Fig. 6: that is, the ends of the curves stop at the positions on the boundary where the meniscus starts, where the temperature is not relevant to the definition of $\overline{\mathrm{Nu}}$. Intersection with the dashed line indicates $\overline{\mathrm{Nu}}$ blow-up, marked with red circles on the graph.

Acknowledgements

H. Rodriguez-Broadbent acknowledges support from an EPSRC studentship. D. G. Crowdy acknowledges support from the QJMAM Fund for Applied Mathematics to attend the AIMS-sponsored Nature Inspired Surface Engineering 2019 conference at Stevens University, New Jersey, USA.

References

1. L. S. Lam, M. Hodes and R. Enright, Analysis of Galinstan-based microgap cooling enhancement using structured surfaces, *J. Heat Trans.* **137** (2015) 091003 (10 pages).

2. A. L. Shah and R. K. London, *Laminar Flow Forced Convection in Ducts: A Source Book for Compact Heat Exchanger Analytical Data* (Academic Press, Cambridge, Massachusetts, USA 1971).

3. J. Ou, B. Perot and J. P. Rothstein, Laminar drag reduction in microchannels using ultrahydrophobic surfaces, *Phys. Fluids* **16** (2004) 4635–4643.

4. J. P. Rothstein, Slip on superhydrophobic surfaces, *Ann. Rev. Fluid Mech.* **42** (2010) 89–109.
5. C. Lee, C. H. Choi and C. J. Kim, Superhydrophobic drag reduction in laminar flows: a critical review, *Exp. Fluids* **57** (2016) 176.
6. T. L. Kirk, M. Hodes and D. T. Papageorgiou, Nusselt numbers for Poiseuille flow over isoflux parallel ridges accounting for meniscus curvature, *J. Fluid Mech.* **811** (2017) 315–349.
7. D. Maynes, B. W. Webb, J. Crockett and V. Solovjov, Analysis of laminar slip-flow thermal transport in microchannels with transverse rib and cavity structured superhydrophobic walls at constant heat flux, *J. Heat Trans.* **135** (2013) 021701 (10 pages).
8. D. Maynes and J. Crockett, Apparent temperature jump and thermal transport in channels with streamwise rib and cavity featured superhydrophobic walls at constant heat flux, *J. Heat Trans.* **136** (2014) 011701.
9. M. Sbragaglia and A. Prosperetti, A note on the effective slip properties for microchannel flows with ultrahydrophobic surfaces, *Phys. Fluids* **19** (2007) 043603.
10. D. G. Crowdy, Analytical formulae for longitudinal slip lengths over unidirectional superhydrophobic surfaces with curved menisci, *J. Fluid Mech.* **791** (2016) R7.
11. A Sander H. and R. G. H. Lammertink, Heat and mass transfer over slippery, superhydrophobic surfaces, *Phys. Fluids*, **28** (2016) 042002.
12. J. R. Philip, Flows satisfying mixed no-slip and no-shear conditions, *Z. fur Angew. Math. Phys*. **23** (1972) 353–372.
13. M. Hodes, L. Steigerwalt Lam, A. Cowley, R. Enright and S. MacLachlan, Effect of evaporation and condensation at menisci on apparent thermal slip, *J. Heat Transfer* **137** (2015) 071502 (7 pages).
14. C.-O. Ng and C. Y. Wang, Temperature jump coefficient for superhydrophobic surfaces, *J. Heat Transfer*, **136** (2014) 064501 (6 pages).
15. D. G. Crowdy, Superhydrophobic annular pipes: a theoretical study, *J. Fluid Mech.* **906** (2021) A15.
16. L. N. Tao, The second fundamental problem in heat transfer of laminar forced convection, *J. Appl. Mech.* **29** (1962) 415–420.
17. T. L. Bergman, F. P. Incropera, D. P. DeWitt and A. S. Lavine, *Fundamentals of Heat and Mass Transfer*, chapter 8 (Wiley, Hoboken, New Jersey, USA 2011).
18. R. Enright, M. Hodes, T. Salamon and Y. Muzychka, Isoflux Nusselt number and slip length formulae for superhydrophobic microchannels, *J. Heat Trans.* **136** (2014) 012402.
19. F. W. J. Olver, A. B. Olde Daalhuis, D. W. Lozier, B. I. Schneider, R. F. Boisvert, C. W. Clark, B. R. Miller, B. V. Saunders, H. S. Cohl and M. A. McClain, eds., *NIST Digital Library of Mathematical Functions*. http://dlmf.nist.gov/, Release 1.1.5 of 2022-03-15.
20. S. Game, M. Hodes, T. Kirk and D. T. Papageorgiou, Nusselt numbers for Poiseuille flow over isoflux parallel ridges for arbitrary meniscus curvature, *J. Heat Trans.* **140** (2018) 081701 (13 pages).
21. M. G. Arun, D. Dilip and S. K. Ranjith, Effect of interface curvature on isothermal heat transfer in a hydrophobic microchannel with transverse ribs and cavities. *Int. J. Therm. Sci.* **167** (2021) 107014.
22. G. Karamanis, *Nusselt Numbers for Superhydrophobic Microchannels and Shrouded Longitudinal-Fin Heat Sinks*. Ph.D. Thesis (Tufts University, Medford, Massachusetts, USA 2018).
23. G. Karamanis, M. Hodes, T. Kirk and D. T. Papageorgiou, Nusselt numbers for fully-developed flow between parallel plates with one plate textured with isothermal parallel ridges, *Heat*

Transfer Summer Conference, vol. 50329 (American Society of Mechanical Engineers, Washington DC, USA 2016) V001T05A004.

24. J. R. Philip, Integral properties of flows satisfying mixed no-slip and no-shear conditions, *Z. fur Angew. Math. Phys*. **23** (1972) 960–968.

25. E. M. Sparrow, B. R. Baliga and S. V. Patankar, Forced convection heat transfer from a shrouded fin array with and without tip clearance, *J. Heat Transfer* **100** (1978) 572–579.

A. Solving for the temperature field

Here, we solve for $T(z, \bar{z})$, detailing the method summarised in section 3. The governing equations are

$$\nabla^2 T = Pw, \tag{A. 1}$$

with

$$\frac{\partial T}{\partial n} = \begin{cases} -1 & \text{for } |z| = 1, \, |\arg(z^m)| < \theta \\ \\ 0 & \text{for } |z| = 1, \, |\arg(z^m)| > \theta. \end{cases} \tag{A. 2}$$

In terms of the complex variable z this is

$$4\frac{\partial^2 T}{\partial z \partial \bar{z}} = Pw \tag{A. 3}$$

with, noting the complex form of the inward normal,

$$-2\mathrm{Re}\left[z\frac{\partial T}{\partial z}\right] = \begin{cases} -1 & \text{for } |z| = 1, \, |\arg(z^m)| < \theta \\ \\ 0 & \text{for } |z| = 1, \, |\arg(z^m)| > \theta. \end{cases} \tag{A. 4}$$

The following decomposition of T is useful:

$$T(z, \bar{z}) = T_f(z, \bar{z}) + g(z) + \overline{g(z)}, \tag{A. 5}$$

where, using the form for $w(z, \bar{z})$ found previously, T_f satisfies

$$4\frac{\partial^2 T_f}{\partial z \partial \bar{z}} = \frac{P}{4}\left(1 - z\bar{z} + f(z) + \overline{f(z)}\right), \tag{A. 6}$$

and $g(z)$ is a holomorphic function determined by the boundary conditions. Integrating this gives

$$T_f(z, \bar{z}) = \frac{P}{16}\left(z\bar{z} - \frac{z^2\bar{z}^2}{4} + \bar{z}F(z) + z\overline{F(z)}\right), \tag{A. 7}$$

where

$$F(z) = \int_0^z f(\hat{z}) d\hat{z}. \tag{A. 8}$$

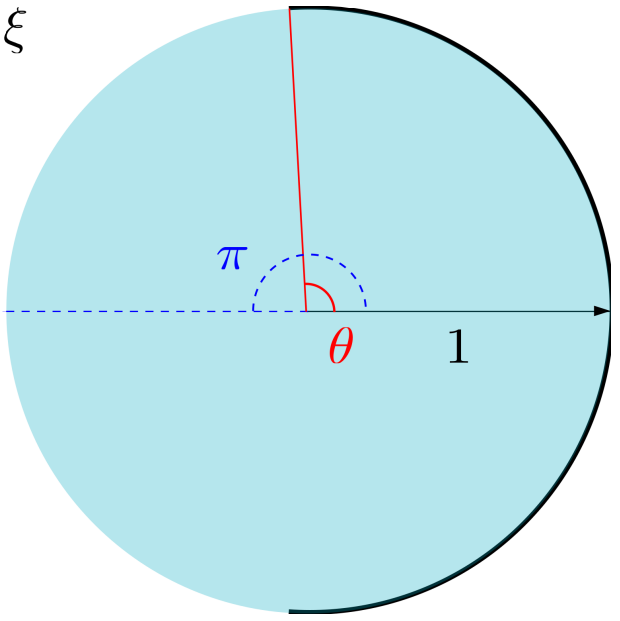

Fig. A.1 The transformed domain in the ξ plane, illustrating the definition of θ.

On substituting the expression (A. 5) into the boundary conditions (A. 4), we have that

$$\mathrm{Re}\left[2z\frac{\partial T_f}{\partial z}+2zg'(z)\right]=\begin{cases}1 & \text{for } |z|=1,\ |\arg(z^m)|<\theta\\ 0 & \text{for } |z|=1,\ |\arg(z^m)|>\theta.\end{cases} \tag{A. 9}$$

With the known form of $T_f(z,\bar{z})$, and using the fact that $z\bar{z}=1$ on the boundary, this reduces the problem to finding a holomorphic function $g(z)$ satisfying, in terms of the transformed coordinate $\xi=z^m$,

$$\mathrm{Re}\left[2\xi(z)g'(\xi(z))\right]=\begin{cases}\dfrac{1}{m}-\dfrac{P}{8m}\mathrm{Re}\left[\left(\dfrac{1}{2}+f(z)+z\overline{F(z)}\right)\right] & \text{for } |\xi(z)|=1,\ |\arg(\xi(z))|<\theta\\ -\dfrac{P}{8m}\mathrm{Re}\left[\left(\dfrac{1}{2}+f(z)+z\overline{F(z)}\right)\right] & \text{for } |\xi(z)|=1,\ |\arg(\xi(z))|>\theta.\end{cases} \tag{A. 10}$$

We further decompose $g(z)$ into the sum of two terms

$$g(z)=g_1(z)+g_2(z), \tag{A. 11}$$

where (henceforth omitting the dependence of ξ on z)

$$\mathrm{Re}[2\xi g_1'(\xi)]=\begin{cases}\dfrac{1}{m} & \text{for } |z|=1,\ |\arg(\xi)|<\theta,\\ 0 & \text{for } |z|=1,\ |\arg(\xi)|>\theta,\end{cases} \tag{A. 12}$$

and

$$\mathrm{Re}[2zg_2'(z)] = -\frac{P}{8}\mathrm{Re}\left[\left(\frac{1}{2} + f(z) + z\overline{F(z)}\right)\right], \qquad \text{on all of } |z| = 1. \tag{A. 13}$$

Notice that it is more useful to work in ξ for $g_1(z)$, and in z for $g_2(z)$. To solve for $g_1(z)$, we let

$$\chi(\xi) = \frac{(\xi - b)(1 - \bar{b})}{(b - 1)(\xi - \bar{b})}, \qquad b = e^{i\theta}, \tag{A. 14}$$

which, as a conformal map, transplants the slotted pipe to the upper half plane, the no-slip region to the negative real axis, and the no-shear boundary portion to the positive real axis. Then, since we require

$$\begin{aligned} \mathrm{Re}\left[2\xi g_1'(\xi)\right] &= \begin{cases} 1/m & \text{for } |\xi| = 1, |\arg(\xi)| < \theta \\ 0 & \text{for } |\xi| = 1, |\arg(\xi)| > \theta. \end{cases} \\ &= \begin{cases} 1/m & \chi \text{ on negative real axis} \\ 0 & \chi \text{ on positive real axis,} \end{cases} \end{aligned} \tag{A. 15}$$

a suitable form is found to be

$$\begin{aligned} \xi g_1'(\xi) &= -\frac{i}{2\pi m}\log\chi = -\frac{i}{2\pi m}\log\frac{(\xi - b)(1 - \bar{b})}{(b - 1)(\xi - \bar{b})} \\ \implies g_1'(\xi) &= -\frac{i}{2\pi m}\left(\frac{\log(\xi - b)}{\xi} - \frac{\log(\xi - \bar{b})}{\xi} + \frac{1}{\xi}\log\frac{1 - \bar{b}}{b - 1}\right) \\ &= -\frac{i}{2\pi m}\frac{1}{\xi}\left(\log\frac{\xi - b}{b} - \log\frac{\xi - \bar{b}}{\bar{b}} + i\theta\right) \\ \implies g_1(z) &= -\frac{i}{2\pi m}\left(\mathrm{Li}_2\left(z^m e^{i\theta}\right) - \mathrm{Li}_2\left(z^m e^{-i\theta}\right)\right) + \frac{\theta}{2\pi}\log z, \end{aligned} \tag{A. 16}$$

where $\mathrm{Li}_2(z)$ is the polylogarithmic function of order 2, or dilogarithm (**19**). Note the logarithmic singularity at $z = 0$, which we expect to be removed by a corresponding term in $g_2(z)$.

As for $g_2(z)$, using the fact that $\mathrm{Re}[z\overline{F(z)})] = \mathrm{Re}\,[\bar{z}F(z)]$, and $\bar{z} = 1/z$ on the unit circle, (A. 13) can be rewritten as

$$\mathrm{Re}\left[2zg_2'(z)\right] = -\frac{P}{8}\mathrm{Re}\left[\frac{1}{2} + f(z) + \frac{F(z)}{z}\right], \qquad \text{on } |z| = 1. \tag{A. 17}$$

The term in square brackets resembles a holomorphic function now. Motivated by this, we seek a function g_2 satisfying

$$\begin{aligned} g_2'(z) &= -\frac{P}{16}\left(\frac{1}{2z} + \frac{f(z)}{z} + \frac{F(z)}{z^2}\right) + \frac{ic}{z}, \qquad c \in \mathbb{R} \\ &= -\frac{P}{16}\left(\frac{1}{2z} + \frac{\frac{d}{dz}(zF(z))}{z^2}\right) + \frac{ic}{z}, \end{aligned} \tag{A. 18}$$

where the constant c is arbitrary due to the freedom given by the real part taken in (A. 17). On integration,

$$\begin{aligned} g_2(z) &= -\frac{P}{16}\left(\frac{1}{2}\log z + \frac{F(z)}{z} - f(0) + 2\int_0^z \frac{F(\hat{z})}{\hat{z}^2}d\hat{z}\right) + ic\log z \\ &= -\frac{P}{16}\left(\frac{1}{2}\log z - \frac{F(z)}{z} + f(0) + 2\int_0^z \frac{f(\hat{z})}{\hat{z}}d\hat{z}\right) + ic\log z \\ &= -\frac{P}{16}\left(\left(\frac{1}{2} + 2f(0) + ic\right)\log z - \frac{F(z)}{z} + f(0) + 2\int_0^z \frac{f(\hat{z}) - f(0)}{\hat{z}}d\hat{z}\right). \end{aligned} \tag{A. 19}$$

Note that T is defined up to a constant, so the constant of integration has been taken such that $T(0) = 0$. We must now chose c to cancel the logarithmic singularity in $g_1(z)$. For this, consider the energy balance equation (derived from the statement of the divergence theorem for T in the cross-sectional domain)

$$\begin{aligned} \frac{P\pi}{8}\left(1 + 4\mathrm{Re}[f(0)]\right) = PQ = \iint_{|z|<1} PwdA = \iint_{|z|<1} \nabla^2 TdA = -\oint_{|z|=1} \frac{\partial T}{\partial n}ds = 2\theta \\ \implies P = \frac{16\theta}{\pi\left(1 - \frac{8}{m}\log\sin\frac{\theta}{2}\right)}. \end{aligned} \tag{A. 20}$$

Therefore,

$$g_1(z) \sim \frac{P}{16}\left(\frac{1}{2} + 2\mathrm{Re}[f(0)]\right)\log z \text{ as } z \to 0, \tag{A. 21}$$

where we have used (A. 20) to substitute for P. In order to cancel the logarithmic singularities in g_1 and g_2 on addition, we choose

$$c = -2\mathrm{Im}[f(0)] = 0, \tag{A. 22}$$

so that

$$\begin{aligned} g_2(z) &= -\frac{P}{16}\left(\frac{1}{2}\left(1 + 4\mathrm{Re}[f(0)]\right)\log z - \frac{F(z)}{z} + f(0) + 2\int_0^z \frac{f(\hat{z}) - f(0)}{\hat{z}}d\hat{z}\right) \\ &= \frac{\theta}{2\pi}\log z + \frac{P}{16}\left(\frac{F(z)}{z} - f(0) - 2\int_0^z \frac{f(\hat{z}) - f(0)}{\hat{z}}d\hat{z}\right). \end{aligned} \tag{A. 23}$$

Finally, we find

$$g(z) = \frac{i}{2\pi m}\left(\mathrm{Li}_2\left(z^m e^{-i\theta}\right) - \mathrm{Li}_2\left(z^m e^{i\theta}\right)\right) + \frac{P}{16}\left(\frac{F(z)}{z} - f(0) - 2\int_0^z \frac{f(\hat{z}) - f(0)}{\hat{z}}d\hat{z}\right). \tag{A. 24}$$

The final expression for the temperature field is then

$$\begin{aligned} T(z,\bar{z}) = \frac{P}{16}\left(z\bar{z} - \frac{z^2\bar{z}^2}{4} + \bar{z}F(z) + z\overline{F(z)}\right) \\ + \mathrm{Re}\left[\frac{i}{\pi m}\left(\mathrm{Li}_2\left(z^m e^{-i\theta}\right) - \mathrm{Li}_2\left(z^m e^{i\theta}\right)\right) + \frac{P}{8}\left(\frac{F(z)}{z} - f(0) - 2\int_0^z \frac{f(\hat{z}) - f(0)}{\hat{z}}d\hat{z}\right)\right]. \end{aligned} \tag{A. 25}$$

B. Integral calculations using Stokes' theorem

This appendix shows how the complex form of Stokes' theorem as stated in (4.5) can be used to calculate integrals over the pipe cross-section—specifically, the mass flux rate Q and the enthalpy flux rate H—without performing any 2D integrals.

The mass flux rate Q is

$$Q = \iint_{|z|<1} w dA = \iint_{|z|<1} \frac{1}{4}(1 - z\bar{z} + f(z) + \overline{f(z)}) dA. \tag{B. 1}$$

On the pipe boundary $\bar{z} = 1/z$, so we can use Stokes theorem to write

$$\iint_{|z|<1} \frac{1}{4}(1 - z\bar{z} + f(z)) dA = \frac{1}{2i} \oint_{|z|=1} \frac{1}{4} \left(\frac{1}{2z} + \frac{f(z)}{z} \right) dz = \frac{\pi}{4} \left(\frac{1}{2} + f(0) \right), \tag{B. 2}$$

and

$$\iint_{|z|<1} \frac{1}{4} \overline{f(z)} dA = -\frac{1}{2i} \oint_{|z|=1} \frac{1}{4} z \overline{f(z)} d\bar{z} = -\frac{1}{8i} \oint_{|z|=1} \frac{\overline{f(z)}}{\bar{z}} d\bar{z} = \overline{\frac{1}{8i} \oint_{|z|=1} \frac{f(z)}{z} dz} = \frac{\pi}{4} \overline{f(0)}. \tag{B. 3}$$

Adding (B. 2) and (B. 3), it follows from (B. 1) that

$$Q = \frac{\pi}{8} (1 + 4\mathrm{Re}[f(0)]). \tag{B. 4}$$

On use of (3.4),

$$f(0) = -\frac{2}{m} \log \sin \frac{\theta}{2}, \tag{B. 5}$$

so it follows that

$$Q(\theta, m) = \frac{\pi}{8} \left(1 - \frac{8}{m} \log \sin \frac{\theta}{2} \right). \tag{B. 6}$$

This result matches that found by Philip (**24**).

Next consider the enthalpy flux rate given by

$$H = \iint_{|z|<1} wT dA = \iint_{|z|<1} wT_f dA + \iint_{|z|<1} w(g + \bar{g}) dA := H_1 + H_2, \tag{B. 7}$$

where we have named the two integrals H_1 and H_2. After application of Stokes' theorem it follows, by steps akin to those used above for Q, that

$$\begin{aligned} H_1 =& \frac{P}{64} \frac{1}{2i} \oint_{|z|=1} \left(\frac{1}{2} z\bar{z}^2 - \frac{5}{12} z^2 \bar{z}^3 + \frac{1}{16} z^3 \bar{z}^4 \right) dz \\ &- \frac{P}{64} \frac{1}{2i} \oint_{|z|=1} \left(\frac{1}{2} z^2 \overline{F(z)} - \frac{1}{3} z^3 \bar{z} \overline{F(z)} + \frac{1}{2} z^2 \bar{z} \overline{f(z)} - \frac{1}{12} z^3 \bar{z}^2 \overline{f(z)} + \frac{1}{2} z^2 \overline{f(z) F(z)} + \bar{z} \overline{f(z)} \Psi(z) \right) d\bar{z} \\ &+ \frac{P}{64} \frac{1}{2i} \oint_{|z|=1} \left(\frac{1}{2} \bar{z}^2 F(z) - \frac{1}{3} z\bar{z}^3 F(z) + \frac{1}{2} z\bar{z}^2 f(z) - \frac{1}{12} z^2 \bar{z}^3 f(z) + \frac{1}{2} \bar{z}^2 f(z) F(z) + z f(z) \overline{\Psi(z)} \right) dz, \end{aligned} \tag{B. 8}$$

where

$$\Psi(z) = \int_0^z F(s)ds. \tag{B. 9}$$

Then, using the fact that $\bar{z} = 1/z$ on the boundary, and noting that the second and third integrals are complex conjugates, this simplifies to

$$\begin{aligned} H_1 =& \frac{P}{64}\frac{1}{2i}\oint_{|z|=1}\frac{7}{48z}dz + \frac{P}{32}\mathrm{Re}\left[\frac{1}{2i}\oint_{|z|=1}\left(\frac{F(z)}{6z^2}+\frac{5f(z)}{12z}+\frac{1}{2z^2}f(z)F(z)+zf(z)\overline{\Psi(z)}\right)dz\right]. \\ =& \frac{P}{64}\left(\frac{7\pi}{48}+2\mathrm{Re}\left[\frac{\pi F'(0)}{6}+\frac{5\pi f(0)}{12}\right. \right. \\ & \left. \left. +\frac{\pi}{2}\left(f'(0)F(0)+f(0)F'(0)\right)+\frac{1}{2i}\oint_{|z|=1} zf(z)\overline{\Psi(z)}dz\right]\right). \end{aligned} \tag{B. 10}$$

Conveniently, $F'(z) = f(z)$, and the $f(0)$ terms can be simplified as before. Also, by taking all indefinite integrals along radial paths starting at the origin, we have that $F(0) = 0$. Then, collecting the integral into the real part of a single term gives:

$$\begin{aligned} H_1 &= \frac{P\pi}{64}\left(\frac{7}{48}+2\mathrm{Re}\left[\frac{7f(0)}{12}+\frac{1}{2}f(0)^2+\frac{1}{2\pi i}\oint zf(z)\overline{\Psi(z)}dz\right]\right) \\ &= \frac{P\pi}{64}\left(\frac{7}{48}+\frac{7}{6}f(0)+f(0)^2+2\mathrm{Re}\left[\mathrm{Res}\left(zf(z)\overline{\Psi(z)}dz;\, z=0\right)\right]\right). \end{aligned} \tag{B. 11}$$

It remains to determine the residue of $zf(z)\overline{\Psi(z)}$ at 0. Note that $f(z)$ and $\Psi(z)$ are holomorphic their Taylor series are as follows:

$$f(z) = \sum_{n=0}^{\infty} a_n z^{mn} \implies F(z) = \sum_{n=0}^{\infty}\frac{a_n}{mn+1}z^{mn+1} \implies \Psi(z) = \sum_{n=0}^{\infty}\frac{a_n}{(mn+1)(mn+2)}z^{mn+2}, \tag{B. 12}$$

where the coefficients a_n can be determined by using the standard result from complex analysis

$$a_n = \frac{1}{2\pi i}\oint_{|z|=1}\frac{f(z)}{z^{n+1}}dz. \tag{B. 13}$$

With this, $\overline{\Psi(z)}$ can be rewritten on the boundary as:

$$\overline{\Psi(z)} = \overline{\Psi}\left(\frac{1}{z}\right) = \sum_{n=0}^{\infty}\frac{\overline{a_n}}{(mn+1)(mn+2)}\left(\frac{1}{z}\right)^{mn+2}. \tag{B. 14}$$

Then, also on the boundary, we have

$$zf(z)\overline{\Psi(z)} = \sum_{n=0}^{\infty}\sum_{k=0}^{\infty}\frac{a_n\overline{a_k}}{(mn+1)(mn+2)}z^{mn-mk-1}, \tag{B. 15}$$

which admits

$$\mathrm{Res}\left(zf(z)\overline{\Psi(z)};\, z=0\right) = \sum_{n=0}^{\infty}\frac{a_n\overline{a_n}}{(mn+1)(mn+2)}. \tag{B. 16}$$

This implies

$$H_1 = \frac{P\pi}{64}\left(\frac{7}{48} + \frac{7}{6}f(0) + f(0)^2 + 2\sum_{n=0}^{\infty}\frac{|a_n|^2}{(mn+1)(mn+2)}\right), \tag{B. 17}$$

and noting that $a_0 = f(0)$, this can be written as

$$H_1 = \frac{P\pi}{64}\left(\frac{7}{48} + \frac{7}{6}f(0) + 2f(0)^2 + 2\sum_{n=1}^{\infty}\frac{|a_n|^2}{(mn+1)(mn+2)}\right). \tag{B. 18}$$

We turn now to H_2. Stokes' theorem can be used to write

$$\begin{aligned} H_2 =& \frac{1}{2}\mathrm{Re}\left[\frac{1}{2i}\oint_{|z|=1}\left(\bar{z}g(z) - \frac{z^2\bar{z}g(z)}{2} + \bar{z}f(z)g(z) + \overline{F(z)}g(z)\right)dz\right] \\ =& \frac{1}{2}\mathrm{Re}\left[\frac{1}{2i}\oint_{|z|=1}\left(\frac{g(z)}{2z} + \frac{f(z)g(z)}{z} + \overline{F(z)}g(z)\right)dz\right] \\ =& \frac{1}{2}\mathrm{Re}\left[\frac{1}{2i}\oint_{|z|=1}\left(\overline{F(z)}g(z)\right)dz\right], \end{aligned} \tag{B. 19}$$

where we have used the residue theorem and the fact that $g(0) = 0$ to arrive at the final line. Since

$$\mathrm{Li}_2(z) = \sum_{n=1}^{\infty}\frac{z^n}{n^2}, \tag{B. 20}$$

incorporating the Taylor expansion for $f(z)$ with (A. 24), we have that

$$g(z) = \sum_{n=0}^{\infty}c_n z^n = \sum_{n=1}^{\infty}\left(\frac{\sin n\theta}{\pi mn^2}z^{mn} - \frac{Pa_n(mn+2)}{16mn(mn+1)}z^{mn}\right) \tag{B. 21}$$

and noting that (B. 12) gives that on the unit circle

$$\overline{F(z)} = \sum_{n=0}^{\infty}\frac{\overline{a_n}}{mn+1}z^{-(mn+1)}, \tag{B. 22}$$

we have that

$$\overline{F(z)}g(z) = \sum_{n=0}^{\infty}\sum_{k=0}^{\infty}\frac{\overline{a_n}c_k}{mn+1}z^{mk-mn-1}, \tag{B. 23}$$

similarly yielding that

$$\mathrm{Res}\left(\overline{F(z)}g(z); z=0\right) = \sum_{n=0}^{\infty}\frac{\overline{a_n}c_n}{mn+1}. \tag{B. 24}$$

Use of the residue theorem simplifies (B. 19) to

$$H_2 = 2\mathrm{Re}\left[\frac{\pi}{4}\sum_{n=0}^{\infty}\frac{\overline{a_n}c_n}{mn+1}\right]. \tag{B. 25}$$

Then, at last, adding (B. 18) and (B. 25), we have

$$H = \frac{P\pi}{64}\left(\frac{7}{48} + \frac{7}{6}f(0) + 2f(0)^2 + 2\sum_{n=1}^{\infty}\frac{|a_n|^2}{(mn+1)(mn+2)}\right) + \frac{\pi}{2}\sum_{n=0}^{\infty}\frac{\mathrm{Re}\,[\overline{a_n}c_n]}{mn+1}. \tag{B. 26}$$

Using the explicit form for c_n, per (B. 21), and noting that a_n are all real,

$$\begin{aligned} H =& \frac{P\pi}{64}\left(\frac{7}{48} + \frac{7}{6}f(0) + 2f(0)^2\right) \\ &+ \sum_{n=1}^{\infty}\left(\frac{a_n \sin n\theta}{2mn^2(mn+1)} - \frac{P\pi a_n^2}{32}\frac{3mn+4}{mn(mn+1)^2(mn+2)}\right) \end{aligned} \tag{B. 27}$$

Written even more explicitly, using (3.9), this is

$$\begin{aligned} H =& \frac{\theta}{4\left(1 - \frac{8}{m}\log\sin\frac{\theta}{2}\right)}\left(\frac{7}{48} - \frac{7}{3m}\log\sin\frac{\theta}{2} + \frac{8}{m^2}\left(\log\sin\frac{\theta}{2}\right)^2\right) \\ &+ \sum_{n=1}^{\infty}\left(\frac{a_n \sin n\theta}{2mn^2(mn+1)} - \frac{\theta a_n^2}{2\left(1 - \frac{8}{m}\log\sin\frac{\theta}{2}\right)}\frac{3mn+4}{mn(mn+1)^2(mn+2)}\right). \end{aligned} \tag{B. 28}$$

It is clear from their functional form that the Taylor coefficients decay algebraically in n, at order $1/m^2n^2$. Since the terms of H outside the series are typically of order 10^{-1}, only a small number of terms are required to see convergence at machine accuracy in practice. Indeed, for 99% accuracy, no more than three terms need be used.

C. Asymptotic analysis

This appendix shows how to derive the result in section 6. In the limit $m \to \infty$, we look at the problem in terms of coordinate (r, ϕ), where $z = re^{i\phi}$. As we expect ϕ variations to be small as $m \to \infty$, we seek an outer solution $w_{\mathrm{outer}}(r)$, satisfying

$$\nabla^2 w_{\mathrm{outer}} = \frac{1}{r}\frac{d}{dr}\left(r\frac{d}{dr}w_{\mathrm{outer}}\right) = -1 \text{ in } r < 1 \tag{C. 1}$$

with

$$\frac{dw_{\mathrm{outer}}}{dr}(0) = 0, \qquad w_{\mathrm{outer}}(1) = \lambda, \tag{C. 2}$$

where λ is a constant slip velocity that remains to be determined. These are satisfied by

$$w_{\mathrm{outer}}(r) = \frac{1}{4}(1 - r^2) + \lambda. \tag{C. 3}$$

Notice that this also satisfies the Navier-slip condition

$$w_{\mathrm{outer}}(1) = -\frac{\lambda}{2}\frac{\partial w_{\mathrm{outer}}}{\partial r}. \tag{C. 4}$$

In order to study the ϕ variation in the flow the velocity problem is now rephrased in terms of the repeating sector of the pipe: that is,

$$\nabla^2 w = \frac{1}{r}\frac{\partial}{\partial r}\left(r\frac{\partial w}{\partial r}\right) + \frac{1}{r^2}\frac{\partial^2 w}{\partial \phi^2} = -1 \text{ in } r < 1, |\phi| < \frac{\pi}{m} \tag{C. 5}$$

with conditions on $r = 1$

$$\begin{aligned} w = \frac{\partial w}{\partial \phi} &= 0 \text{ on } |\phi| < \frac{\theta}{m}, \\ \frac{\partial w}{\partial r} &= 0 \text{ on } \frac{\theta}{m} < |\phi| < \frac{\pi}{m}, \\ \frac{\partial w}{\partial \phi} &= 0 \text{ on } |\phi| = \frac{\pi}{m}. \end{aligned} \tag{C. 6}$$

Defining 'inner variables' (R, Φ) with $\epsilon = 1/m$, namely,

$$r = 1 - \epsilon R \qquad \phi = \epsilon \Phi \qquad w_{\text{inner}}(R, \Phi) = \epsilon W_1(R, \Phi) + \epsilon^2 W_2(R, \Phi) + \ldots, \tag{C. 7}$$

and noting that

$$\frac{\partial}{\partial r} = -\frac{1}{\epsilon}\frac{\partial}{\partial R} \qquad \frac{\partial}{\partial \phi} = \frac{1}{\epsilon}\frac{\partial}{\partial \Phi}$$

$$\frac{1}{r} = 1 + \epsilon R + \epsilon^2 R^2 + \ldots \qquad \frac{1}{r^2} = 1 + 2\epsilon R + 3\epsilon^2 R^2 + \ldots,$$

(C. 5) becomes

$$\begin{aligned} &(1 + \epsilon R + \epsilon^2 R^2 + \ldots)\left(-\frac{1}{\epsilon}\right)\frac{\partial}{\partial R}\left[(1 - \epsilon R)\left(-\frac{1}{\epsilon}\right)\frac{\partial}{\partial R}(\epsilon W_1 + \epsilon^2 W_2 + \ldots)\right] \\ &\quad + (1 + 2\epsilon R + 3\epsilon^2 R^2 + \ldots)\frac{1}{\epsilon^2}\frac{\partial^2}{\partial \Phi^2}[\epsilon W_1 + \epsilon^2 W_2 + \ldots] = -1 \\ &\implies (1 + \epsilon R + \ldots)\frac{\partial}{\partial R}\left[(1 - \epsilon R)\frac{\partial}{\partial R}(W_1 + \epsilon W_2 + \ldots)\right] \\ &\quad + (1 + 2\epsilon R + \ldots)\frac{\partial^2}{\partial \Phi^2}[W_1 + \epsilon W_2 + \ldots] = -\epsilon, \end{aligned} \tag{C. 8}$$

so that, at leading order,

$$\frac{\partial^2 W_1}{\partial R^2} + \frac{\partial^2 W_1}{\partial \Phi^2} = 0 \text{ at } O(1). \tag{C. 9}$$

The required boundary conditions for the inner problem are

$$\begin{aligned} W_1 = \frac{\partial W_1}{\partial \Phi} &= 0 \text{ on } |\Phi| < \theta, R = 0, \\ \frac{\partial W_1}{\partial R} &= 0 \text{ on } \theta < |\Phi| < \pi, R = 0, \\ \frac{\partial W_1}{\partial \Phi} &= 0 \text{ on } |\Phi| = \pi, \end{aligned} \tag{C. 10}$$

together with the matching condition

$$\begin{aligned}\lim_{R\to\infty}\frac{\partial w_{\text{inner}}}{\partial R} &= \lim_{r\to 1}\frac{\partial w_{\text{outer}}}{\partial R}\\ &= -\lim_{r\to 1}\epsilon\frac{\partial}{\partial r}\frac{\partial w_{\text{outer}}}{\partial r} = \frac{\epsilon}{2}\\ \implies w_{\text{inner}} &\sim \lambda + \epsilon\frac{R}{2}\ \text{as}\ R\to\infty.\end{aligned} \tag{C. 11}$$

This imposes a shear condition on the inner problem:

$$\frac{\partial W_1}{\partial R} = \frac{1}{2}\ \text{as}\ R\to\infty, \tag{C. 12}$$

while also giving means to link back to the outer solution through the constant λ. These equations are now analogous to Philip's (1972) equations for the difference between the flow over a flat plate with periodic longitudinal no-shear menisci with far-field shear, and pure shear flow as if over a meniscus-free plate ($X\mapsto\Phi$, $Y\mapsto R$, $\tau_\infty/\mu = 1/2$, $w_3\mapsto W_1$) (**12**). Philip shows that this has the solution, in terms of complex variable $\mathcal{Z} = \Phi + iR$,

$$W_1 = \text{Im}\left[\cos^{-1}\left\{\frac{\cos\frac{\pi+\mathcal{Z}}{2}}{\cos\frac{\pi-\theta}{2}}\right\}\right]. \tag{C. 13}$$

Note that the additional π's to the $\mathcal{Z}$'s correspond to transforming the orientation of Philip's problem statement to ours (that is, a rotation of half the ridge period in the pipe). Then, we notice that

$$W_1 \sim \frac{R}{2} - \log\sin\frac{\theta}{2}\ \text{as}\ R\to\infty, \tag{C. 14}$$

and therefore the matching condition determines our slip velocity

$$\lambda = -\epsilon\log\sin\frac{\theta}{2}. \tag{C. 15}$$

Considering the zero boundary conditions for the higher order problems, we find that

$$W_n \equiv 0\ \text{for}\ n\geqslant 2, \tag{C. 16}$$

and therefore

$$\begin{aligned}w_{\text{asymptotic}} :=& w_{\text{inner}} + w_{\text{outer}} - \lim_{R\to\infty} w_{\text{inner}}\\ =& \frac{1}{4}(1-r^2) + \epsilon\,\text{Im}\left[\cos^{-1}\left\{\frac{\cos\frac{\pi+\mathcal{Z}}{2}}{\cos\frac{\pi-\theta}{2}}\right\} - \frac{1}{2}(\pi+\mathcal{Z})\right]\\ :=& w_0(r) + \epsilon w_1(\mathcal{Z}).\end{aligned} \tag{C. 17}$$

We then notice that

$$z = re^{i\phi} = (1-\epsilon R)e^{i\epsilon\Phi} \implies z^m = \left(1-\frac{R}{m}\right)^m e^{i\Phi} \to e^{-R}e^{i\Phi} = e^{i\mathcal{Z}}\ \text{as}\ m\to\infty. \tag{C. 18}$$

Hence,

$$i(\pi + \mathcal{Z}) = \log\left(-z^m\right) \implies \frac{\pi + \mathcal{Z}}{2} = -\frac{im}{2}\log(-z). \tag{C. 19}$$

Substituting this into $w_{\text{asymptotic}}$, with $r^2 = z\bar{z}$, gives the composite solution

$$\begin{aligned} w(z,\bar{z}) &= \frac{1}{4}(1 - z\bar{z}) + \frac{1}{m}\text{Im}\left[\cos^{-1}\left\{\frac{\cos\left(-\frac{im}{2}\log((-1)^{1/m}z)\right)}{\cos\frac{\pi-\theta}{2}}\right\} + \frac{im}{2}\log((-1)^{1/m}z)\right] \\ &= \frac{1}{4}(1 - z\bar{z}) + \epsilon\text{Im}\left[\cos^{-1}\left\{\frac{\sin\left(\frac{i}{2}\log(z^{1/\epsilon})\right)}{\sin\frac{\theta}{2}}\right\} + \frac{i}{2}\log(z^{1/\epsilon})\right], \end{aligned} \tag{C. 20}$$

which matches (3.2).

Equation (C. 18) indicates exponential accuracy in this limit. It also illustrates that this adjustment term due to the superhydrophobicity differs between the pipe and plate problems by the conformal map $e^{\mathcal{Z}}$. Considering these terms are both solutions to Laplace's equations with conformally equivalent boundary conditions, this is unsurprising.

We now turn to the temperature problem. Noting that (3.9) becomes

$$P = \frac{16\theta}{\pi}(1 + 8\epsilon\log\sin\frac{\theta}{2} + \dots), \tag{C. 21}$$

seek a radial outer temperature profile

$$T_{\text{outer}}(r) = \tau_0(r) + \epsilon\tau_1(r) + O(\epsilon^2), \tag{C. 22}$$

satisfying (2.8), together with the outer velocity (C. 3): that is,

$$\frac{1}{r}\frac{d}{dr}\left(r\frac{d}{dr}(\tau_0 + \epsilon\tau_1)\right) = \frac{16\theta}{\pi}\left(1 + 8\epsilon\log\sin\frac{\theta}{2}\right)\left(w_0 - \epsilon\log\sin\frac{\theta}{2}\right) + O(\epsilon^2) \tag{C. 23}$$

noting that the remaining contribution from the velocity to the right hand side is asymptotically small in the outer region. This gives that the leading order temperature satisfies

$$\frac{1}{r}\frac{d}{dr}\left(r\frac{d\tau_0}{dr}\right) = \frac{4\theta}{\pi}(1 - r^2) \tag{C. 24}$$

with

$$\frac{d\tau_0}{dr}(0) = 0. \tag{C. 25}$$

As in the exact problem, we also enforce (without loss of generality) that $\tau_0(0) = 0$, giving

$$\tau_0(r) = \frac{\theta}{\pi}r^2\left(1 - \frac{r^2}{4}\right). \tag{C. 26}$$

Moving next to first order, we have that

$$\frac{1}{r}\frac{d}{dr}\left(r\frac{d\tau_1}{dr}\right) = \frac{16\theta}{\pi}\left(\log\sin\frac{\theta}{2}\right)(1 - 2r^2) \tag{C. 27}$$

with

$$\frac{d\tau_1}{dr}(0) = 0. \tag{C. 28}$$

This similarly gives that

$$\tau_1(r) = \frac{4\theta}{\pi}\left(\log\sin\frac{\theta}{2}\right) r^2\left(1 - \frac{r^2}{2}\right), \tag{C. 29}$$

and so combining these yields that

$$T_{\text{outer}}(r) = \frac{\theta}{\pi} r^2\left(1 - \frac{r^2}{4} + 4\epsilon\left(\log\sin\frac{\theta}{2}\right)\left(1 - \frac{r^2}{2}\right)\right) + O(\epsilon^2). \tag{C. 30}$$

Moving again to the inner region, we seek

$$T_{\text{inner}}(R, \Phi) = T_0(R, \Phi) + \epsilon T_1(R, \Phi), \tag{C. 31}$$

where

$$\nabla^2 T_{\text{inner}} = P w_{\text{inner}}, \tag{C. 32}$$

which implies that

$$\begin{aligned}(1 + \epsilon R + \dots)\frac{\partial}{\partial R}\left[(1 - \epsilon R)\frac{\partial}{\partial R}(T_0 + \epsilon T_1 + \dots)\right] \\ +(1 + 2\epsilon R + \dots)\frac{\partial^2}{\partial \Phi^2}[T_0 + \epsilon T_1 + \dots] = \epsilon^3 P(W_1 + \epsilon W_2 + ...),\end{aligned} \tag{C. 33}$$

that is, at leading two orders

$$\frac{\partial^2 T_n}{\partial R^2} + \frac{\partial^2 T_n}{\partial \Phi^2} = 0 \text{ at } O(1), \text{ for } n = 0, 1, \tag{C. 34}$$

together with the relevant boundary conditions: the heat flux condition along the solid boundary is given by

$$\frac{\partial}{\partial r}(T_0 + \epsilon T_1 + ...) = \begin{cases} -1 & \text{for } R = 0, |\Phi + 2\pi n| < \theta \\ 0 & \text{for } R = 0, \theta < |\Phi + 2\pi n| < \pi, \end{cases} \tag{C. 35}$$

for $n \in \mathbb{Z}$, and changing variables gives that

$$\frac{\partial}{\partial R}(T_0 + \epsilon T_1 + ...) = \begin{cases} \epsilon & \text{for } R = 0, |\Phi + 2\pi n| < \theta \\ 0 & \text{for } R = 0, \theta < |\Phi + 2\pi n| < \pi. \end{cases} \tag{C. 36}$$

Conservation of energy in a period window within the inner region gives the far field condition

$$\begin{aligned}&\frac{\partial}{\partial R}(T_0 + \epsilon T_1 + ...) \to \epsilon\frac{\theta}{\pi} \text{ as } R \to \infty \\ \implies &(T_0 + \epsilon T_1 + ...) \sim \sigma + \epsilon\frac{\theta}{\pi} R \text{ as } R \to \infty,\end{aligned} \tag{C. 37}$$

where σ is a constant to be determined. These conditions are satisfied at order ϵ^0 by

$$T_0 \equiv \sigma, \tag{C. 38}$$

and at order ϵ^1 by T_1 such that

$$\frac{\partial^2 T_1}{\partial R^2} + \frac{\partial^2 T_1}{\partial \Phi^2} = 0, \tag{C. 39}$$

with

$$\frac{\partial T_1}{\partial R} = \begin{cases} 0 & \text{for } R = 0, |\Phi + 2\pi n| < \theta \\ 1 & \text{for } R = 0, \theta < |\Phi + 2\pi n| < \pi, \end{cases} \tag{C. 40}$$

and

$$T_1 \sim \frac{\theta}{\pi} R \text{ as } R \to \infty. \tag{C. 41}$$

To solve this, first define $\hat{T}_1$ such that

$$T_1 = \frac{\theta}{\pi} R + \hat{T}_1, \tag{C. 42}$$

so that we are now seeking a $\hat{T}_1$ that still solves Laplace's equation, now with boundary conditions

$$\frac{\partial \hat{T}_1}{\partial R} = \begin{cases} -\dfrac{\theta}{\pi} & \text{for } R = 0, |\Phi + 2\pi n| < \theta \\ 1 - \dfrac{\theta}{\pi} & \text{for } R = 0, \theta < |\Phi + 2\pi n| < \pi \\ 0 & \text{as } R \to \infty. \end{cases} \tag{C. 43}$$

Note that $\hat{T}_1$ must be the real part of a holomorphic function. We denote

$$\hat{T}_1(\mathcal{Z}, \overline{\mathcal{Z}}) = p(\mathcal{Z}) + \overline{p(\mathcal{Z})}, \tag{C. 44}$$

where $p(\mathcal{Z})$ is a holomorphic function. The required boundary conditions are now that

$$2\mathrm{Re}\left[ip'(\mathcal{Z})\right] = \begin{cases} -\dfrac{\theta}{\pi} & \text{for } R = 0, |\Phi + 2\pi n| < \theta \\ \dfrac{\pi - \theta}{\pi} & \text{for } R = 0, \theta < |\Phi + 2\pi n| < \pi \\ 0 & \text{as } R \to \infty. \end{cases} \tag{C. 45}$$

These are all satisfied by

$$\begin{aligned} 2\mathrm{Re}\left[ip'(\mathcal{Z})\right] &= -\frac{\theta}{\pi} - \frac{1}{\pi}\mathrm{Re}\left[i \log \frac{\sin\frac{\mathcal{Z}+\theta}{2}}{\sin\frac{\mathcal{Z}-\theta}{2}} \right] \\ \implies p'(\mathcal{Z}) &= \frac{\theta}{2\pi} i - \frac{1}{2\pi} \log \frac{\sin\frac{\mathcal{Z}+\theta}{2}}{\sin\frac{\mathcal{Z}-\theta}{2}}. \end{aligned} \tag{C. 46}$$

To integrate, we note the general result

$$\int \log \sin x dx = -\frac{i}{2}x^2 + \left(\frac{i\pi}{2} - \log 2\right)x + \frac{i}{2}\mathrm{Li}_2\left(e^{2ix}\right) + \text{constant}, \tag{C. 47}$$

which gives, after an appropriate choice of arbitrary constant,

$$p(\mathcal{Z}) = \frac{i}{2\pi}\left(\mathrm{Li}_2(e^{i(\mathcal{Z}+\theta)}) - \mathrm{Li}_2(e^{i(\mathcal{Z}-\theta)})\right). \tag{C. 48}$$

Therefore, substituting this back into the inner temperature gives

$$T_{\text{inner}}(R, \Phi) = \sigma + \epsilon\left(\frac{\theta}{\pi}R - \frac{1}{\pi}\mathrm{Im}\left[\mathrm{Li}_2(e^{i(\mathcal{Z}+\theta)}) - \mathrm{Li}_2(e^{i(\mathcal{Z}-\theta)})\right]\right) + O(\epsilon^2). \tag{C. 49}$$

Considering matching, since

$$\lim_{r\to 1} T_{\text{outer}} = -\frac{3\theta}{4\pi} \qquad\qquad \lim_{r\to 1}\frac{\partial T_{\text{outer}}}{\partial R} = \epsilon\frac{\theta}{\pi} \tag{C. 50}$$

it is clear that the first condition determines $\sigma = -3\theta/4\pi$, and the second is readily satisfied thanks to energy conservation. Then, noting that $z^m = e^{i\mathcal{Z}}$, we arrive at the composite solution

$$\begin{aligned} T(z,\bar{z}) =& \frac{\theta}{\pi}z\bar{z}\left(1 - \frac{z\bar{z}}{4}\right) \\ &+ \epsilon\left(\frac{4\theta}{\pi}\left(\log\sin\frac{\theta}{2}\right)z\bar{z}\left(1-\frac{z\bar{z}}{2}\right) - \frac{1}{\pi}\mathrm{Im}\left[\mathrm{Li}_2(z^{1/\epsilon}e^{i\theta}) - \mathrm{Li}_2(z^{1/\epsilon}e^{-i\theta})\right]\right) \\ &+ O(\epsilon^2), \end{aligned} \tag{C. 51}$$

agreeing with (3.11) up to $O(\epsilon)$. Now that we have the velocity and temperature fields up to $O(\epsilon)$, we continue by seeking the first-order correction to the Nusselt number in this large m limit. First, we consider the correction to the mixing cup temperature. To facilitate this, we write

$$w(z,\bar{z}) = \frac{1}{4}(1 - z\bar{z}) + \epsilon\left(a(z) + \overline{a(z)}\right), \tag{C. 52}$$

where $a(z) = mf(z)$,

$$T(z,\bar{z}) = \frac{\theta}{\pi}z\bar{z}\left(1 - \frac{z\bar{z}}{4} + 4\epsilon\left(\log\sin\frac{\theta}{2}\right)\left(1-\frac{z\bar{z}}{2}\right)\right) + \epsilon\left(b(z) + \overline{b(z)}\right) + O(\epsilon^2), \tag{C. 53}$$

where $b(z) = p(\mathcal{Z}(z))$, and

$$H = h_0 + \epsilon h_1 + O(\epsilon^2). \tag{C. 54}$$

The complex form of Stokes' theorem gives, at leading order,

$$h_0 = \iint_{|z|<1}\frac{\theta}{4\pi}z\bar{z}(1-z\bar{z})\left(1-\frac{z\bar{z}}{4}\right)dA = \frac{\theta}{8\pi i}\oint_{|z|=1}\left(\frac{z\bar{z}^2}{2} - \frac{5z^2\bar{z}^3}{12} + \frac{z^3\bar{z}^4}{16}\right)dz = \frac{7\theta}{192}, \tag{C. 55}$$

and, at the next order,

$$\begin{aligned}
h_1 =& \iint_{|z|<1} \left(\frac{\theta}{\pi} z\bar{z} \left(1 - \frac{z\bar{z}}{4}\right) \left(a(z) + \overline{a(z)}\right) \right. \\
&\left. + \frac{1}{4}(1 - z\bar{z}) \left(\frac{4\theta}{\pi} \left(\log \sin \frac{\theta}{2} \right) z\bar{z} \left(1 - \frac{z\bar{z}}{2}\right) + b(z) + \overline{b(z)} \right) \right) dA \\
=& \mathrm{Re}\left[\frac{1}{2i} \oint_{|z|=1} \left\{ \frac{\theta}{\pi} \left(\frac{z\bar{z}^2}{2} - \frac{z^2\bar{z}^3}{12} \right) 2a(z) + \frac{\theta}{\pi} \left(\log \sin \frac{\theta}{2} \right) \left(\frac{z\bar{z}^2}{2} - \frac{z^2\bar{z}^3}{2} + \frac{z^3\bar{z}^4}{8} \right) \right. \right. \\
&\left. \left. + \frac{1}{4} 2b(z) \left(\bar{z} - \frac{z\bar{z}^2}{2} \right) \right\} dz \right] \\
=& \mathrm{Re}\left[\frac{5\theta}{6} a(0) + \frac{\theta}{8} \log \sin \frac{\theta}{2} + \frac{\pi}{4} b(0) \right] \\
=& -\frac{7\theta}{24} \log \sin \frac{\theta}{2},
\end{aligned} \tag{C. 56}$$

where we have used that $a(0) = -\frac{1}{2} \log \sin \frac{\theta}{2}$ and $b(0) = 0$. Next, we consider the mass flux rate

$$Q = \frac{\pi}{8} \left(1 - 8\epsilon \log \sin \frac{\theta}{2}\right), \tag{C. 57}$$

and so the mixing cup temperature is

$$\begin{aligned}
T_b = \frac{H}{Q} &= \left(\frac{7\theta}{192} - \epsilon \frac{7\theta}{24} \log \sin \frac{\theta}{2} \right) \frac{8}{\pi} \left(1 + 8\epsilon \log \sin \frac{\theta}{2}\right) + O(\epsilon^2) \\
&= \frac{7\theta}{24\pi} \left(1 - 8\epsilon \log \sin \frac{\theta}{2}\right) \left(1 + 8\epsilon \log \sin \frac{\theta}{2}\right) + O(\epsilon^2) = \frac{7\theta}{24\pi} + O(\epsilon^2),
\end{aligned} \tag{C. 58}$$

which, interestingly, features no first-order correction. Consequently, the Nusselt number, for z on the no-slip region, is

$$\begin{aligned}
\mathrm{Nu}(z) &= 2 \left(\frac{3\theta}{4\pi} + \epsilon \left(\frac{2\theta}{\pi} \left(\log \sin \frac{\theta}{2} \right) - \frac{1}{\pi} \mathrm{Im}\left[\mathrm{Li}_2(z^{1/\epsilon} e^{i\theta}) - \mathrm{Li}_2(z^{1/\epsilon} e^{-i\theta}) \right] \right) - \frac{7\theta}{24\pi} \right)^{-1} + O(\epsilon^2) \\
&= \frac{48\pi}{11\theta} \left(1 - \epsilon \frac{24}{11} \left(2 \log \sin \frac{\theta}{2} + \frac{1}{\theta} \mathrm{Im}\left[\mathrm{Li}_2(z^{1/\epsilon} e^{i\theta}) - \mathrm{Li}_2(z^{1/\epsilon} e^{-i\theta}) \right] \right) \right) + O(\epsilon^2) \\
&= \frac{48\pi}{11\theta} - \epsilon \frac{1152\pi}{121\theta} \left(2 \log \sin \frac{\theta}{2} + \frac{1}{\theta} \mathrm{Im}\left[\mathrm{Li}_2(z^{1/\epsilon} e^{i\theta}) - \mathrm{Li}_2(z^{1/\epsilon} e^{-i\theta}) \right] \right) + O(\epsilon^2),
\end{aligned} \tag{C. 59}$$

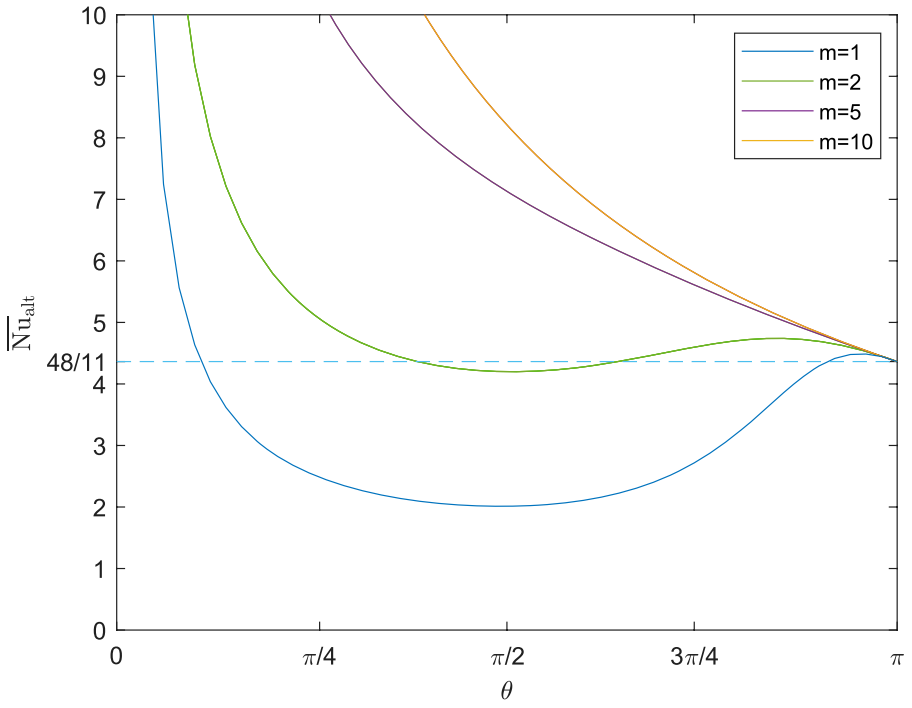

Fig. D.1 Alternative average Nusselt number, $\overline{\mathrm{Nu}}_{\mathrm{alt}}$, as a function of solid ridge angle θ: again calculated with 10 terms in the series for H truncated.

and, on taking an average, we find

$$\begin{aligned}\overline{\mathrm{Nu}} &= \frac{1}{2\pi\epsilon}\int_{-\epsilon\theta}^{\epsilon\theta}\mathrm{Nu}(e^{i\phi})d\phi \\ &= \frac{48}{11} - \epsilon\frac{2304}{121}\log\sin\frac{\theta}{2} - \frac{576}{121\theta^2}\mathrm{Im}\left[\int_{-\epsilon\theta}^{\epsilon\theta}\left(\mathrm{Li}_2(e^{i\phi/\epsilon}e^{i\theta}) - \mathrm{Li}_2(e^{i\phi/\epsilon}e^{-i\theta})\right)d\phi\right] + O(\epsilon^2) \\ &= \frac{48}{11} - \epsilon\frac{2304}{121}\log\sin\frac{\theta}{2} + \epsilon\frac{576}{121\theta^2}\mathrm{Im}\left[i\int_{e^{-i\theta}}^{e^{i\theta}}\left(\mathrm{Li}_2(te^{i\theta}) - \mathrm{Li}_2(te^{-i\theta})\right)\frac{dt}{t}\right] + O(\epsilon^2) \\ &= \frac{48}{11} + \epsilon\frac{576}{121}\left(\frac{1}{\theta^2}\mathrm{Re}\left[\mathrm{Li}_3(e^{2i\theta}) - 2\mathrm{Li}_3(1) + \mathrm{Li}_3(e^{-2i\theta})\right] - 4\log\sin\frac{\theta}{2}\right) + O(\epsilon^2).\end{aligned} \tag{C. 60}$$

D. Alternate definitions of the Nusselt number

Enright *et al.* (**18**), amongst others, posit an alternative to the Nusselt number as defined in this work. Rather than averaging the local Nusselt number around the solid boundary, they average the solid boundary temperature

and calculate a global Nusselt number with that. As such, defining the alternative average Nusselt number

$$\overline{\mathrm{Nu}}_{\mathrm{alt}} := \frac{2}{\overline{T} - T_b}, \qquad \overline{T} := \frac{1}{2\theta}\int_{-\theta/m}^{\theta/m} T(e^{is})ds, \tag{D. 1}$$

this is plotted in Fig. D1, showing markedly different results to this work.

Most notably this definition suffers from singular behaviour as $\theta \to 0$, while Fig. 3 indicates that $\lim_{\theta\to 0}\overline{\mathrm{Nu}} = 0$. While this limit is explicitly non-physical, as the fluid velocity is unsurprisingly singular as the entire boundary becomes a no-shear surface, making energy balance impossible, some intuition can be gleamed from this. For the original Nusselt number definition (4.3), as the solid boundary arclength vanishes so too does the arclength over with the local Nusselt number is non-zero, making the average Nusselt number the mean of a quantity that is uniformly zero. However, in this alternative definition it is the $\overline{T}$ term that depends on the vanishing solid boundary: in this limit of $\theta \to 0$, it is clear from Fig. 6 that $\overline{T} \to T_b$, and so $\overline{\mathrm{Nu}}_{\mathrm{alt}}$ blows up.

This initial singularity skews the values of the alternative Nusselt number for larger, more physical values of θ, thus making the improvement to a Nusselt number of 48/11 less meaningful. Interestingly, this alternative definition has a local minimum in the $m = 1, 2$ cases, and for some values of θ larger than this minimum we still see that $\overline{\mathrm{Nu}}_{\mathrm{alt}} > 48/11$. However, this quantity's global behaviour is so vastly different to this originally defined Nusselt number that the authors deem this connection to be too tenuous to offer serious corroboration.